IMPACT OF RENEWABLE ENERGY SYSTEMS ON SHORT CIRCUIT LEVELS IN POWER SYSTEM DISTRIBUTION NETWORKS

DISSERTATION

SUBMITTED IN PARTIAL FULFILLMENT OF THE REQUIREMENTS
FOR THE AWARD OF THE DEGREE

OF

MASTER OF TECHNOLOGY
IN
POWER SYSTEMS

Submitted by:

Guru Sharan Singh
(2K14/PSY/09)

Under the supervision of

Dr. Mukhtiar Singh
(Associate Professor)

DEPARTMENT OF ELECTRICAL ENGINEERING
DELHI TECHNOLOGICAL UNIVERSITY
(Formerly Delhi College of Engineering)
Bawana Road, Delhi-110042

2016

DEPARTMENT OF ELECTRICAL ENGINEERING

DELHI TECHNOLOGICAL UNIVERSITY

(Formerly Delhi College of Engineering)

Bawana Road, Delhi-110042

CERTIFICATE

I, Guru Sharan Singh, Roll No. 2K14/PSY/09 student of M. Tech. (Power System), hereby declare that the dissertation/project titled "IMPACT OF RENEWABLE ENERGY SYSTEMS ON SHORT CIRCUIT LEVELS IN POWER SYSTEM DISTRIBUTION NETWORKS" under the supervision of DR. MUKHTIAR SINGH, Associate Professor, Department of Electrical Engineering Department, Delhi Technological University in partial fulfillment of the requirement for the award of the degree of Master of Technology has not been submitted elsewhere for the award of any Degree.

Place: Delhi
Date: 01.08.2016

GURU SHARAN SINGH
2K14/PSY/09

Dr. MUKHTIAR SINGH
(Associate Professor)
Electrical Engineering Department
Delhi Technological University
Bawana Road, Delhi-110042

ACKNOWLEDGEMENT

I would like to express my sincere gratitude to Dr. Mukhtiar Singh for his guidance and assistance in the thesis. The technical discussions with him were always been very insightful, and I will always be indebted to him for all the knowledge he shared with me. His prompt responses and availability despite his constantly busy schedule were truly appreciated. He always helped me in all the technical and non-technical issues during the production of this thesis. Without his consistent support, encouragement and valuable inputs, this project would not have become possible.

I would like to express my deep gratitude to Prof. Madhusudan Singh, Head, Department of Electrical Engineering for providing his support during my project.

I would like to thank Mr. Ashutosh Trivedi for his invaluable and lively discussions during the tenure of this research work.

Finally, I express my deep sincere thanks to my Parents and my brother who motivated and encouraged me for higher studies, without which it wouldn't have been possible.

Guru Sharan Singh
(2K14/PSY/09)
M.Tech (Power System)
Delhi Technological University, Delhi

ABSTRACT

The short circuit analysis secures the electrical power systems protection scheme. Thus, in turn ensures the power system reliability, safe mode of operation, and uninterruptable power supply. The impact of distributed generation on the power systems stability, power quality, and short circuit level is still unclear and uncertain. The different characteristics of each distributed generation type, such as synchronous generators, induction generators, power electronics inverters make it more complicated to assess. Studying the effect of the penetration of distributed generation on fault current level of existing distribution networks is crucial. This thesis will examine the impact of implementing distributed generation mix, including wind turbine generators, photovoltaic, and its combination on the fault current level of the distributed network under study. The short circuit analysis is carried out on the IEEE 37-bus distribution test system using ETAP 12.6 software. The simulation results are presented in a comparison between six cases, comparing the impact of the distributed generation mix on the fault current level at different levels of penetration. Moreover, a comparison showing the contribution of each distributed generation type separately as a percentage is presented. The selection of distributed generation technology and location has a significant impact on the fault current.

CANDIDATE DECLARATION

I, Guru Sharan Singh, Roll No.-2K14/PSY/09 student of M. Tech.(POWER SYSTEM) , hereby declare that the dissertation/project titled **" Impact Of Renewable Energy Systems On Short Circuit Levels In Power System Distribution Networks "** under the supervision of Dr. Mukhtiar Singh, Department of Electrical Engineering, Delhi Technological University, in partial fulfilment of the requirement for the award of the degree of Master of Technology has not been submitted elsewhere for the award of any Degree.

Place: Delhi
Date: 01/08/2016

Guru Sharan Singh
M.Tech (Power System)
2K14/PSY/09
Dept. of Electrical Engineering
DTU, New Delhi

CONTENTS

LIST OF FIGURES

LIST OF TABLES

LIST OF ABBREVIATIONS

C-WET …….. Centre For Wind Energy Technology

WISE..…….. ..World Institute Of Sustainable Energy

STC..…….....Standard Test Condition

FF……Fill factor

SCIG……...Squirrel Cage Induction Generators

DFIG……...Doubly Fed Induction Generators

WRIG……....Wound Rotor Induction Generator

RSC……....Rotor Side Converter

GSC ……...Grid Side Converter

FSC…….....Full Scale Converter

SCL ……Short-Circuit Level

DG……...Distributed generation

IEEE……..…. Institute of Electrical and Electronics Engineers

ETAP……. *Electrical Transient Analyzer Program*

EDS…….Electrical distribution system

SCC…….Short circuit current

MNRE ……Ministry of *New* and *Renewable Energy*

Q……..*Reactive power*

P……..*Active power*

BBC……*Back to Back Converter*

WPD…… …Weibull Probability Distribution

RMF…….Rotating Magnetic Field

SLG……..Single Line To Ground Fault

LLG…… Double Line to Ground Faults

LL……Line to Line

CB……....Circuit Breaker

LN……Line To Neutral

PCC…….Point Of Common Coupling

IM……Induction Machine

P_{MPP}…….Maximum Power Point

I_{MP}…….Maximum Power Point Current

V_{MP}……Maximum Power Point Voltage

TSR……..Tip Speed Ratio

KE……..Kinetic Energy

CHAPTER 1

INTRODUCTION

As a result of human activities, greenhouse gases are increasing at a very fast rate in the earth's atmosphere. Many scientific communities now believe that this increase in carbon dioxide (CO2), methane (CH4), chlorofluorocarbons and other greenhouse gases is causing the earth's temperature to rise, and that this increase in greenhouse gases will lead to even greater global warming. Renewable energy resources like sunlight, wind etc. are clean and environmental friendly. They can provide many immediate environmental benefits by preventing the emission of greenhouse gases and can help in conservation of fossil resources for future generations. Therefore, all over the world government is encouraging the development of renewable energy to limit greenhouse gases in earth's atmosphere.

1.1 INDIAN WIND ENERGY POTENTIAL

MNRE has incorporated Centre for Wind Energy Technology (C-WET) for development and growth of wind energy in India and this agency is responsible for wind resource assessment. Earlier the data of wind potential in India was around 50 GW, but now it is around 105 GW[33] .State wise data of Indian wind energy potential and installation has been shown below in Table 1.1and Table 1.2 respectively[33].Wind resource assessment done by another research institute, World Institute of Sustainable Energy (WISE) shows similar results as C-WET [33].

TABLE 1.1 – STATE WISE WIND ENERGY POTENTIAL

States/UTs	Estimated potential	States / UTs	Estimated potential
Gujarat	35071	Meghalaya	250
Andhra Pradesh	14497	Arunachal Pradesh	236
Tamil Nadu	14152	Bihar	144
Karnataka	13593	Pondicherry	120
Maharashtra	5961	Assam	112
Jammu & Kashmir	5685	Sikkim	98
Rajasthan	5050	Jharkhand	91
Orissa	1384	Meghalaya	82
Madhya Pradesh	2931	Himachal Pradesh	64
Uttar Pradesh	1260	Manipur	56
Kerala	837	West Bengal	22
Uttarakhand	534	Nagaland	16
Andaman & Nicobar	365	Lakshadeep	16
Chhattisgarh	314	Daman and Diu	4
Total			**102788**

TABLE 1.2 - STATE WISE WIND ENERGY INSTALLATION IN INDIA

States / UTs	Installed capacity	Percentage of total installation
Tamil Nadu	7276	34.2%
Maharashtra	4098	19.3%
Gujarat	3414	16.1%
Rajasthan	2820	13.3%
Karnataka	2409	11.3%
Andhra Pradesh	753	3.5%
Madhya Pradesh	439	2.1%
Kerala	55	0.3%
West Bengal	1.1	0.1%
Others	3.2	0.02%
Total	**21268.3**	**100%**

1.2 INDIAN SOLAR ENERGY POTENTIAL

With around 280 clear sky days per year, its calculated solar energy incidence on its land area, is about 5k trillion (kWh). Available energy in a form of solar per year exceeds the all possible energy output from fossil fuel energy reserves in India. The average solar power generation capacity per day over India is 0.25 kWh per m^2 of used land area [32]. Solar power capacity in India, statewise is shown below in figure 1.1[32].

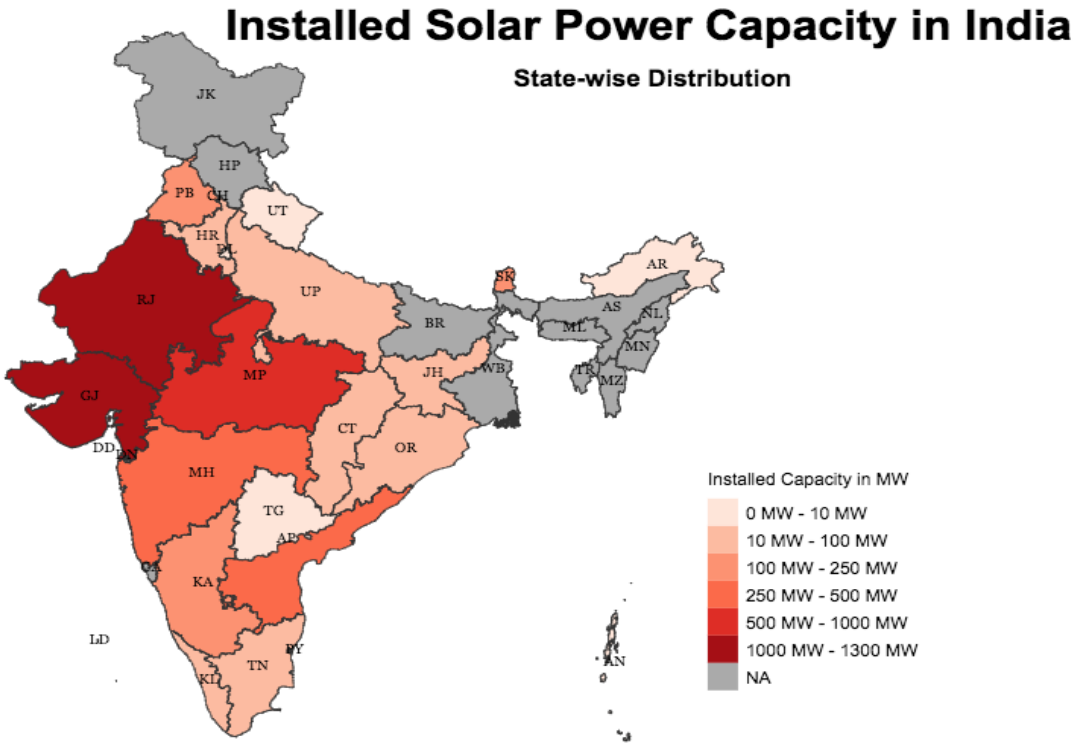

Figure 1.1- Installed Solar Capacity in India.

1.3 PHOTOVOLTAIC OVERVIEW

Photovoltaic systems have become a source of energy for a wide range of applications. The applications could be standalone or grid connected PV systems. A standalone PV system is used in isolated applications where it is connected directly to the load and storage system. In a standalone photovoltaic, when the PV source of energy is very huge, having energy storage is beneficial. Whereas a grid connected PV is used when it injects the current directly into the grid itself. The advantage of the system connected to grid is its ability to sell excess of energy. Figure 1.2 shows a block diagram of typical hybrid renewables sources of energy. The integrated system has PV array and wind turbine as energy source. They are connected to the DC bus through converters that could be connected to a different energy storage system, or inject the current directly with a three phase DC/AC inverter to grid.

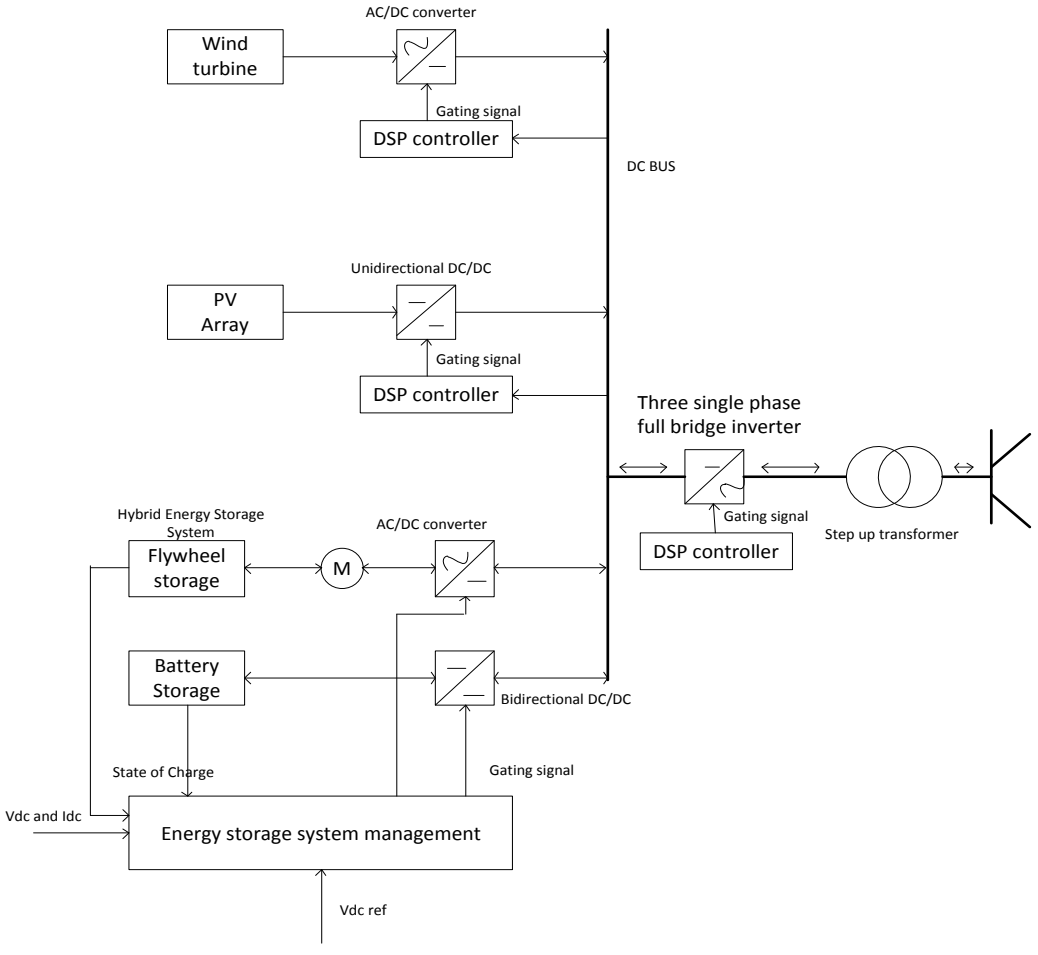

Figure 1.2-Block Diagram of Typical Hybrid Renewables Sources of Energy

1.4 PHOTOVOLTAIC CHARACTERISTICS

1.4.1 Irradiation Effect

Power output of PV is affected by irradiation incident on it. PV module I_{sc} varies linearly with incident irradiation, while V_{oc} increases exponentially to the maximum value with increasing incident irradiation, and it varies slightly with the light intensity. Figure 1.3 describes the relation between photovoltaic current and voltage with the incident irradiation.

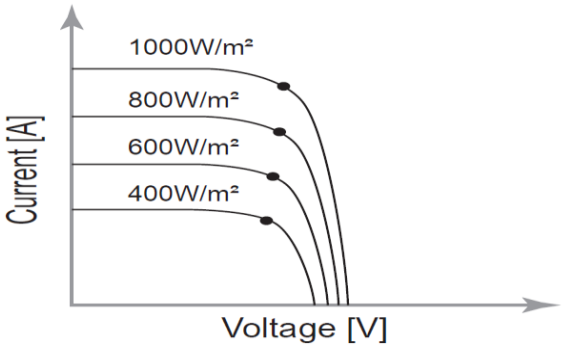

Figure 1.3- Effects of the incident Irradiation on Module Voltage and Current

1.4.2 Temperature Effect

PV module temperature is highly affected by ambient temperature. Short circuit current (I_{sc}) increases slightly when the temperature of the module rises more than the STC temperature, which is 25^{oC}. However the V_{oc} is affected enormously when the module temperature is greater than 25^{oC}. Therefore, power output of the module is reduced. Figure1.4 shown below explains its effect.

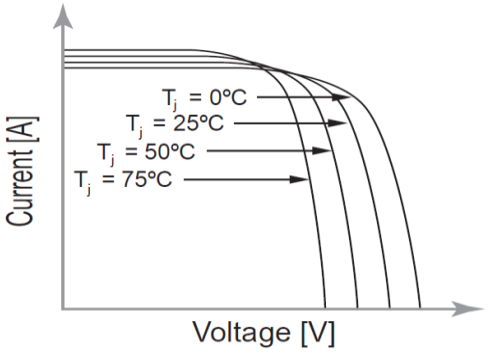

Figure 1.4- Effect of Ambient Temperature on Module Voltage and Current

1.4.3 Maximum Power Point (P_{MPP})

Power output of the module is equal to I_{MP} multiplied by the V_{MP}, which is the maximum possible power available at STC. Referring to Figure 1.5, the "knee" of the I-V curve represents the P_{MPP} of the PV module/system. At this point the maximum electrical power is generated. The usable electrical output power depends on the PV module efficiency which is related to the technology used and manufacture of module.

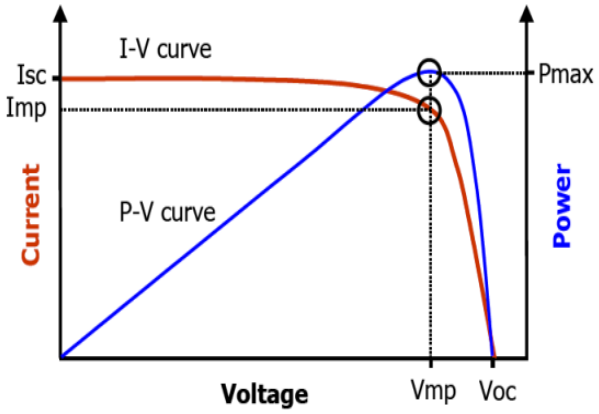

Figure 1.5- Maximum Power Point

1.4.4 -Fill Factor (FF)

FF is an important parameter for PV cell/module; it represents the area of the largest rectangle, which fits in the I-V curve. The importance of fill factor is linked with the magnitude of the output power. The higher the fill factor (FF) higher output power is. Figure 1.6 illustrates the fill factor which is the ratio between the two rectangular areas and is given by the formula shown below. The ideal fill factor (FF) value is 1 which means that the two rectangles are exactly identical.

$$FF = \frac{Imp * Vmp}{Isc * Voc}$$

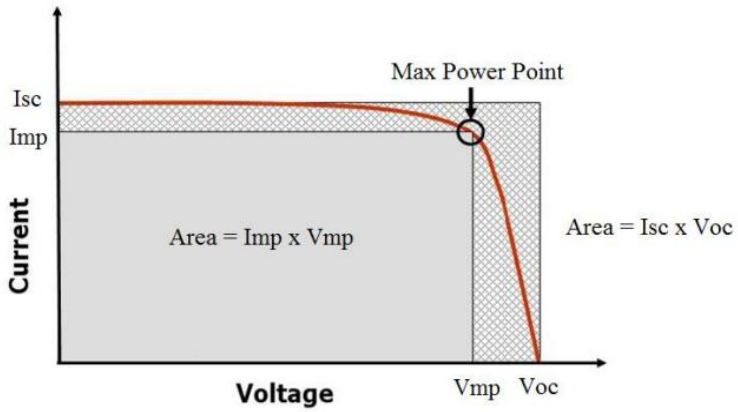

Figure 1.6- Fill Factor

1.4.5 Module Efficiency (η_{PV}):

The PV cell/module efficiency defines its ability to convert sunlight to electricity. Mathematically, it evaluates the output power of the module per unit area and the maximum efficiency of the PV module/cell is given by:

$$\eta_{PVmax} = \frac{Vmp * Imp}{G * A} * 100\%$$

Where G is global radiation and considered to be 1000 W/m^2 at (STC) and A is the Area of the PV module.

1.5 WIND TURBINES OVERVIEW

Commercial classification of wind turbines is basically categorised, based on its operation at fixed speed , variable speed, size and partial and full-scale PEC used. the Most common type of wind turbines is fixed speed. Though it is cheap and simple, it has many disadvantages like it deliver a power to grid which follows fluctuations in wind speed, which results flicker emission as well as high mechanical stress on drive train. Above disadvantages are eliminated in variable-speed(limited) wind turbine. Such type of WTG are able to absorb the fluctuations and convert them to heat and kinectic energy into an external rotor resistance, hence decreasing the grid power fluctuations.

Nowadays majority of WTG installed is variable-speed based which are able to vary shaft speed widely and have capability to extract optimal power at low speeds also. Optimization of power extraction is done keeping the TSR close to optimal value. It also have superior control, reactive power control, frequency control and voltage support.

1.5.1 Fixed-Speed Wind Turbine (TYPE-1)

Type-1 is equipped with a SCIG which directly feeds power to grid via a transformer (step-up), as shown below in figure 1.7 and figure1.8 shows block diagram of Type-1. Because to its torque-slip behaviour, it operates at constant speed almost, having slip around 1-2 % at rated value, which means its speed depends on frequency of grid. We may use soft starter to avoid high current transients during grid interconnection. Because of stiff interconnection to grid, Type-1 cannot absorb the wind power fluctuations. As a result, fluctuations are observed in power and torque. Mechanical stresses is due to torque fluctuations and voltage flicker is due to power fluctuations [26],[34].

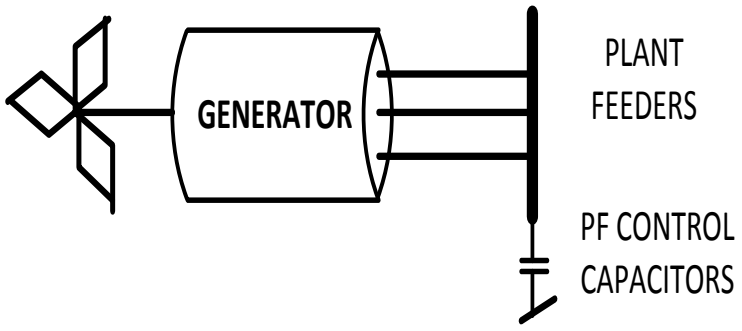

Figure 1.7-Fixed-Speed Turbine with SCIG.

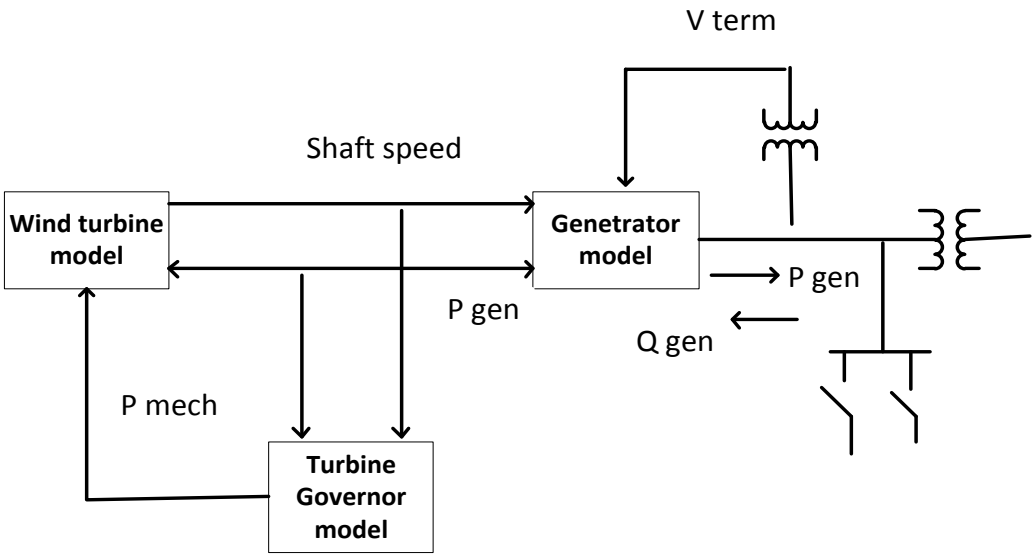

Figure 1.8- Block Diagram of Type-1 Wind Turbine

Capacitors are installed to decrease the reactive power power drawn from grid. However during dip in voltage, the turbine accelerates and draws very high amount of reactive power from grid, which is very high in comparison of normal conditions.

1.5.2-Limited Variable-Speed Wind Turbine (TYPE-2)

In this type of WTG, WRIG is used and a resistance is connected externally to rotor. Value of the resistance (external) is controlled by controlling converter. A scheme and block diagram of such WTG concept is shown below in figure 1.9 and 1.10 respectively. With increase in rotor resistance, the maximum torque of IG is shifted toward high slip and high speed as observed in torque slip curve. Type-2 WTG may operates above the rated speed, with a slip range around 10 %.

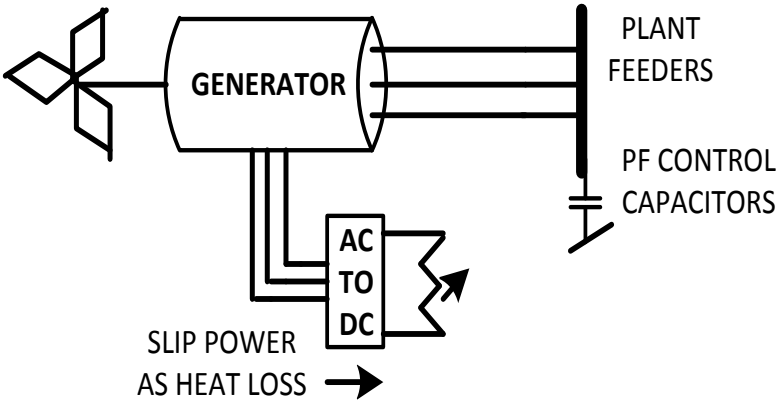

Figure 1.9- Limited Variable-Speed Turbine with WRIG and Variable Resistance Connected to Rotor.

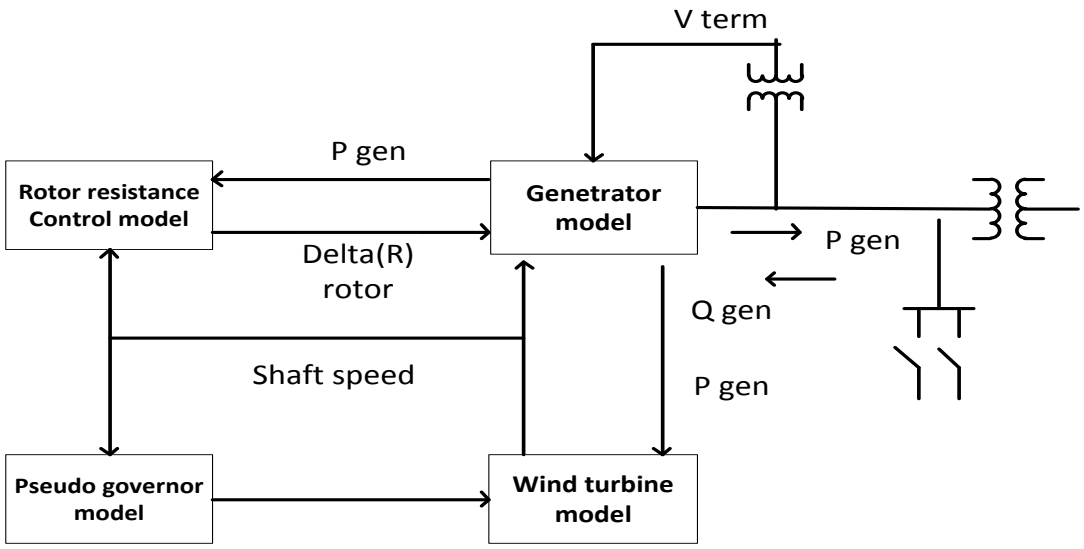

Figure 1.10- Block Diagram of Type-2 Wind Turbine

Range of speed is restricted by the losses in external resistance in the form of heat. Such control strategy is used to absorb power fluctuations (wind) into KE of the turbine shaft and then dissipate it via external resistance in the form of heat. One of the major drawback of type-2 concept is that P and Q cannot be controlled independently. This turbine is like type-1, as it also use capacitor bank as type-2 also draws Q from the grid [26],[34].

1.5.3- (TYPE-3) Variable-Speed Turbine with DFIG

Type-3 wind turbine is a variable speed with (DFIG). In this generator stator is directly connected to grid directly. And rotor interconnection to is via BBC i.e RSC and GSC. Here three winding transformer (step-up) may be used, as shown below in Figure 1.11. Here converter on rotor side is called throughout as RSC, while the converter on grid side as the GSC.

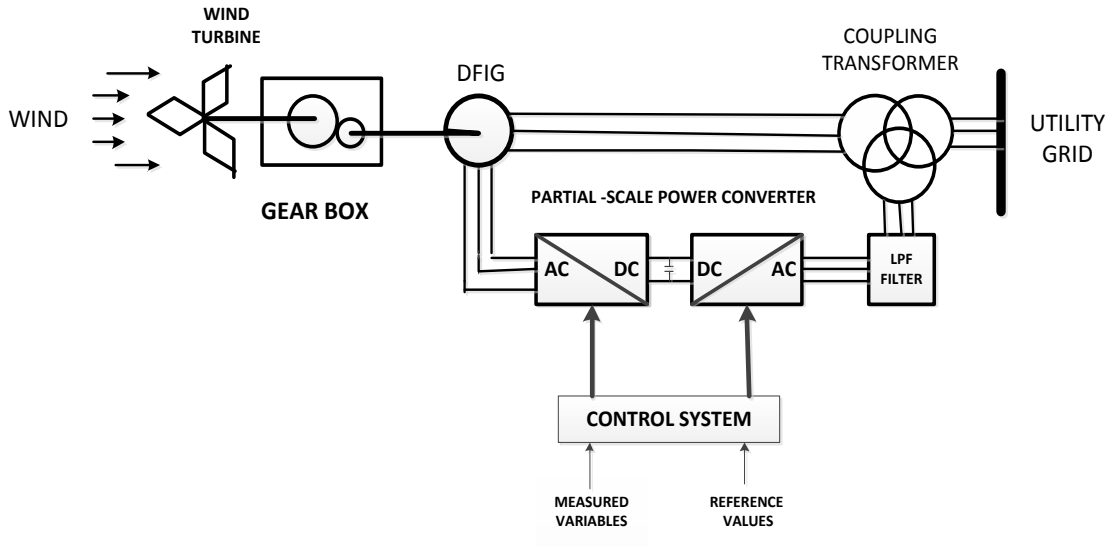

Figure 1.11- Variable-Speed Wind Turbine with DFIG (Type-3)

Bi-directional power flow through rotor as explained in block diagram figure 1.12. When turbine operates at subsynchronous speed, power flows into rotor. Its direction of power flow reverses at super-synchronous speed. Because of high input power (mechanical), some power is fed to grid through stator and some through the BBC converter. RSC is normally controlling the P and Q power injection into grid through stator. Adjusting external voltage which is applied to rotor, P and Q can be independently controlled. By adjusting this voltage, the current can also be controlled in stator to deliver Q to grid.

Because of fast control of RSC it becomes possible to feed P smoothly into grid. By controlling the RSC the wind power extraction at low wind speeds can be optimized.

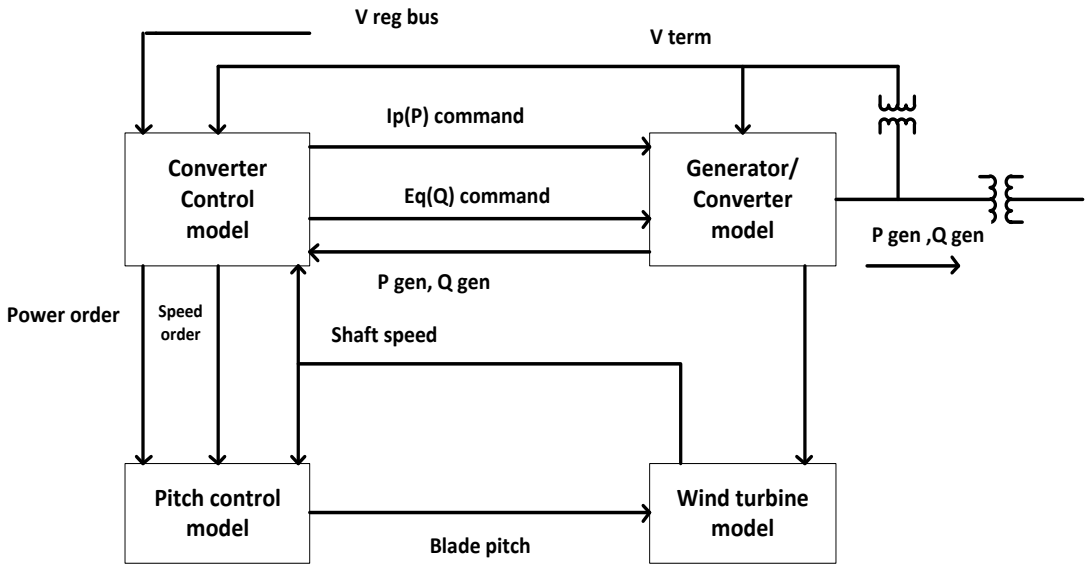

Figure 1.12- Block Diagram of Type-3 Wind Turbine

During normal operation, grid side controller controls the capacitor voltage of DC-link and not contribute(usually) to any exchange of Q from grid. Type-3 wind turbines advantage is that its BBC only needs to be sized to handle approximately 30% of rated power of the generator. This is because, power flows through rotor is expressed as product of stator power and slip and DFIG is operating within a slip around -30% to +30%.

One of the important term is rotor to stator turns ratio, it should be chosen properly to reduce converter current rating. If its value is selected around 3, then the maximum voltage of rotor during normal conditions will be around 1pu. As a result rotor current will not be more than 0.3 pu times of stator current. Sensitiveness to grid disturbances is its major drawback. A voltage dip may result in high current in rotor which may damage RSC, so in these situation RSC switching is blocked [26],[34].

1.5.4-Variable-Speed Wind Turbine with FSC (TYPE-4)

In this type wind turbine concept turbine is connected to grid via FSC as shown below in figure 1.13. The generator can be either of induction or synchronous type. In case of synchronous type, we have two options like separately excited and a permanent magnet synchronous generator. If an IG is used, it needs to be magnetized by GSC. So, it is rated to handle P as well as Q and Q can be supplied by capacitors installed at terminals. To optimize the extracted power from wind, GSC controls speed of generator. Type-4 has a wider speed range for operation than Type-3. GSC controls the capacitor voltage of DC-link feeding P into grid and also controls Q injection independently.

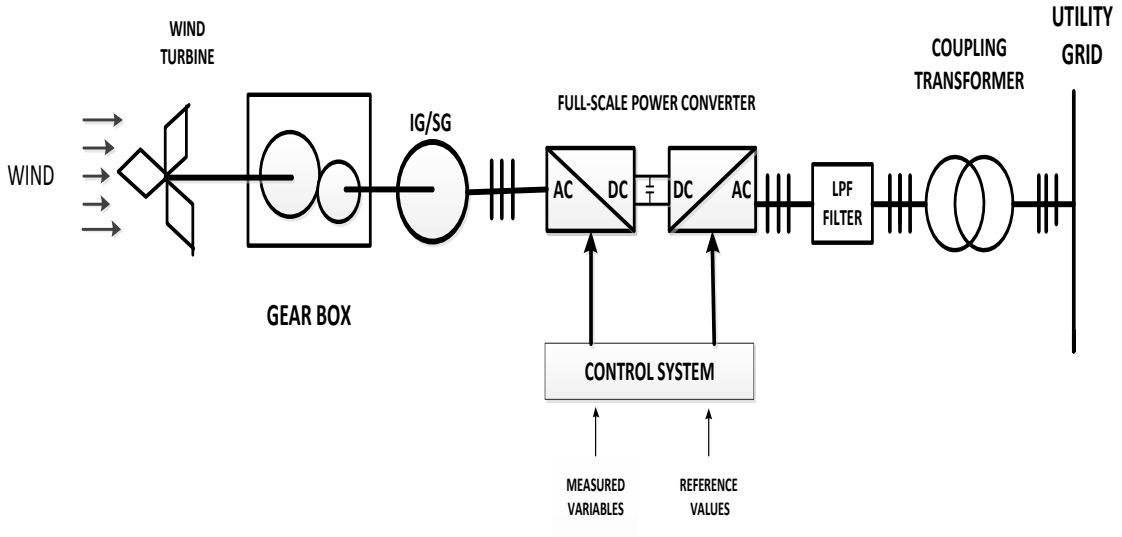

Figure1.13- Variable-Speed Wind Turbine with FSC

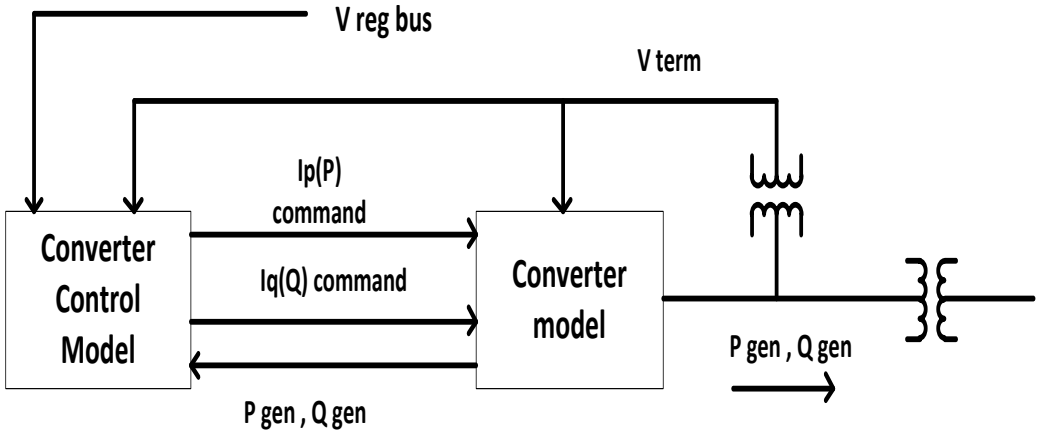

Figure 1.14- Block Diagram of Type-4 WTG

Type-4 turbine having FSC, is easily controlled during voltage dips in respect to DFIG. Here dip in voltage does not cause any transient in generator directly. The main issue of type-4 is rise of capacitor voltage of DC-link when no P delivered to grid. The GSC can also provide fast reactive power support, as explained through block diagram in figure 1.14 [26],[34].

1.6 MODEL OF WIND POWER SYSTEM

A DFIG equivalent model is developed here which is connected to grid. It means that all DFIG cannot be individually modelled, instead 'n' turbines are grouped to represent as a one turbine having output of n*1 MW. This assumption is justified as difference in speeds of wind which incident on each turbine does not cross 2 $m.s^{-1}$. Here model of wind farm model indicates control model, wind model, mechanical model, generator(electrical) model and aerodynamic model [28] as shown below in figure 1.15 and its mathematical modeling is explained in APPENDIX A.

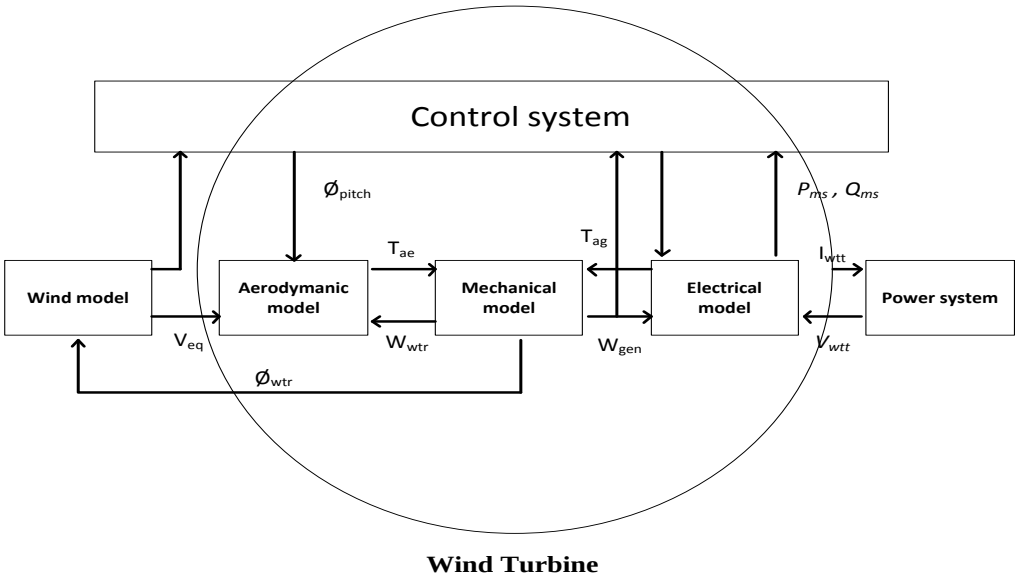

Figure1.15- Different Subsystems of Grid Connected Wind Farm Model

1.6.1 Wind Model

WPD function is used to represent distribution of wind speed at a particular location and by maximum likelihood method we can find parameters 'k' and 'c' if for a particular area wind data is known .The inverse WPD function is here used to produce random numbers is represented by Equation 1.1. Where k represents shaping parameter, c represents scaling parameter ($m.s^{-1}$) and t is sample time.

$$f(t) = \frac{k}{c}\left(\frac{1}{t}\right)^{k+1} e^{-\frac{1}{c}\left(\frac{1}{t}\right)^{k}} \qquad \ldots\ldots\ldots (1.1)$$

1.6.2 Aerodynamic Model

Relationship between energy and wind velocity described by kinetic energy equation as 1.2.

$$E_k = \frac{1}{2}mv^2 \qquad \ldots\ldots\ldots\ldots\ldots\ldots\ldots (1.2)$$

Substitute mass component 'm' from 1.2 as Equation (1.3)

$$m=\rho\Pi R^2 vt \qquad \ldots\ldots\ldots\ldots\ldots\ldots (1.3)$$

where, v(linear velocity of particles), ρ(air density), R(diameter of the rotor)and t(time). Put values from 1.3 into 1.2 to get 1.4 to get total energy content E_k in wind.

$$E_k = \frac{1}{2}\Pi\rho R^2 v^3 t \qquad \ldots\ldots\ldots\ldots (1.4)$$

Dividing Equation (1.4) by t gives the power delivered by wind (P_{wind}) as given below by equation (1.5).

$$P_{wind} = \frac{1}{2}\Pi\rho R^2 v^3 \qquad \ldots\ldots\ldots\ldots (1.5)$$

Equation (1.6) represents power captured by turbine.

$$P_{turb} = \frac{1}{2}\Pi\rho R^2 v^3 C_p\left(\emptyset_{pitch}, \lambda\right) \qquad \ldots\ldots (1.6)$$

C_p depends on pitch angle of blades (θ_{pitch}) and tip speed ratio (λ), given as :

$$\lambda = \frac{\text{tip speed}}{\text{wind speed}} = \frac{w_{turb} R}{v} \qquad \ldots\ldots(1.7)$$

Equation (1.6) shows, for a high value of power a large value of C_p is required. To get a high C_p value which depends on λ and θ_{pitch} so it optimized and process for optimization of these variables is called MPPT. When the angular velocity and power delivered to turbine is known, then applied torque to rotor may be obtained from Equation (1.8).

$$T_{turb} = \frac{\frac{1}{2}\rho \Pi R^2 v^3 C_p(\emptyset_{pitch}, \lambda)}{w_{turb}} \qquad \ldots\ldots\ldots(1.8)$$

1.6.3 Mechanical Model

For this a single lumped model is used for modelling where rotating parts are represented by single mass. The mathematical equations for this is given by equation (1.9)

$$2(H_t + H_r) = \frac{dwr}{dt} = T_t - T_{em} \qquad \ldots..(1.9)$$

Where H_t (inertia constants of turbine), H_r (inertia constants of generator rotor), τ_t(turbine torque) and τ_{em} (electromagnetic torque) and the rotational is represented by ω_r.

1.6.4 DFIG Model

DFIG is basically WRIG whose stator is interconnected to grid directly while rotor is through a BBC. Because of this connection DFIG feeds in two ways (Doubly-Fed) to grid and it also enhances stability of grid as it can also feed Q. The power flow diagram of DFIG is shown earlier in figure-1.11**.**

DFIG can be modelled in two ways (1)- a steady state (2)-dynamic representation of its electrical behaviour. To determine the response of DFIG during disturbances dynamic model is used.

When rotor rotates because of prime mover, a RMF is created in air gap. Due to this RMF voltage is produced(induced) on rotor and stator windings and for this machine

have to continuously rotate at a speed higher than RMF called n_s. The difference between rotor speed and RMF speed is called slip's', which is defined by (1.10) as:

$$s = \frac{n_s - n}{n_s} \quad \text{.....(1.10)}$$

where n_s called synchronous speed and n called rotor speed. And as observed that 's' value is negative when operates as generator. Rotor side voltage frequency is different from that of the stator side and is given by 1.11.

$$f_r = sf_s \quad \text{.....(1.11)}$$

The stator and rotor 'P' is given by (1.12) and (1.13).

$$P_s = T_{em} w_s = \frac{T_m w}{(1-s)} = \frac{P_m}{(1-s)} \quad \text{.....(1.12)}$$

$$P_r = -sP_s \quad \text{.....(1.13)}$$

where ω_s (synchronous velocities), ω (angular velocities of rotor) in rad.s^{-1}, 'm (mechanical) and em(electromagnetic) .

1.7 FAULT ANALYSIS

Protection systems are designed to protect the power system against undesirable operating conditions that result as a fault in the power system network. Faults can occur as a result of lightning, tree flashover, breakdown of insulation or human error. Amongst others, the most common characteristic of fault is a rapid increase of the current to level above normal operating range. Faults can also change the voltage or frequency of the power system network.

Many studies are performed by system planners and operators so that that the power system network is operating correctly. These studies include short-circuit, stability, load flow studies and reliability analysis. SCC analysis is one of the most widely used studies especially when considering protection systems, for which it can provide the values necessary for determining relay settings for coordination of protection devices. Because of this purpose the focus will be on short circuit analysis for fault level calculations.

Short circuit faults may be divided as…

- Symmetrical.
- Unsymmetrical.

1.7.1 Symmetrical Faults

A 3- phase fault is a result of 3 equal fault impedances Z_f of the 3 phases, as shown below in Figure 1.17-1.18. As $Z_f = 0$ fault is called a solid fault. This type of faults may be of 2 types: (a) three phase to ground fault (LLLG fault) or (b) three phase fault (LLL fault). In this all three phases are affected equally, so the system remains balanced. This is why, it is called a symmetrica fault. The behaviour of LLLG fault and LLL fault is same because of balanced nature of fault. This type of fault is a severe fault and if $Z_f = 0$, this is usually the most severe type of fault that may occur in a system. Fortunately, the occurrence of such type of fault is only about 5% of the total system fault.

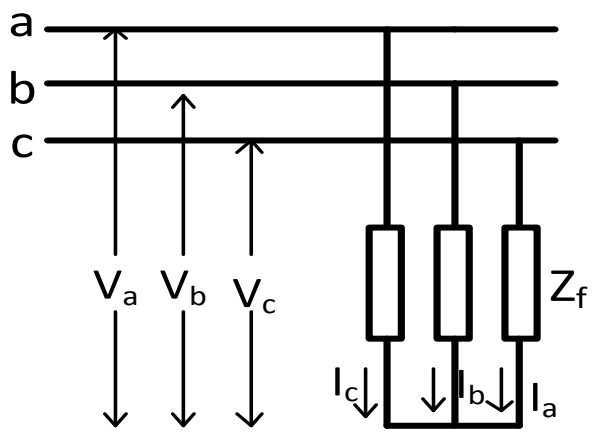

Figure 1.16- Three Phase Fault

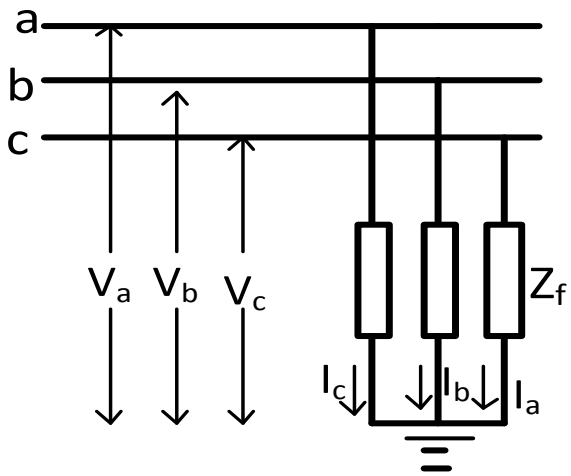

Figure1.17- Three Phase to Ground Fault

1.7.2 Unsymmetrical Faults

The type of faults in which balanced behaviour of system is disturbed are called unsymmetrical faults. SLG fault is most common among this type of fault which is around 60 to 75% of the total faults. Other unbalanced faults are LL fault and LLG fault. Around 15 to 25% - LLG faults and around 5 to 15% - LL faults as shown in table 1.3. These faults are shown in Figure 1.19-1.21.

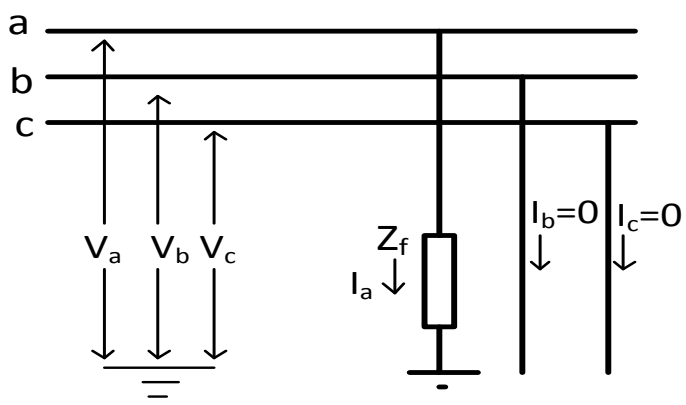

Figure 1.18- Single Line to Ground Fault

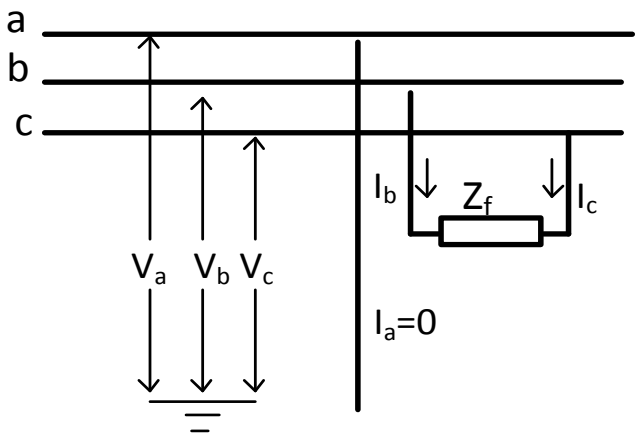

Figure 1.19- Line to Line Fault

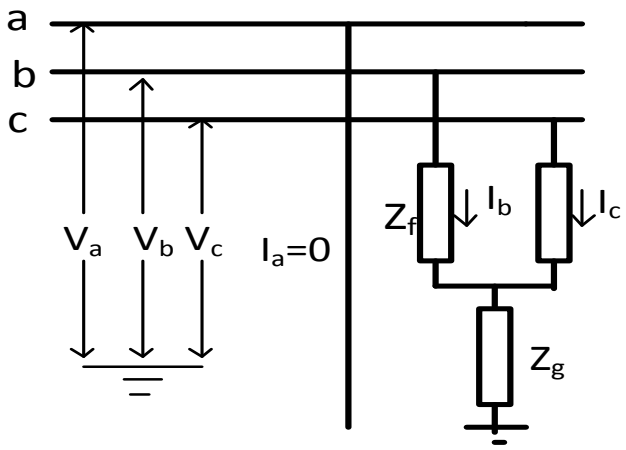

Figure 1.20- Double Line to Ground Fault

TABLE 1.3- OCCURRENCE OF DIFFERENT FAULT

FAULT TYPE	OCCURRENCE
Three Phase to Ground Fault	5-7%
Single Phase to Ground Fault	60 -75 %
Double Phase to Ground	15 - 25 %
Phase to Phase Fault	5 – 15 %

1.8 SHORT CIRCUIT CURRENT

SCC occur when a fault, such as breakdown of insulation, lightning or tree flashover, results in a short circuit between lines or line to ground. It is this current which can damage equipment on the power system and which needs to be detected and prevented by the protection equipment.

The magnitude of the SCC is due to two main components. They are, the equivalent system impedance at the point of fault point, which produces a decaying DC component and the performance of the rotating machinery, which result in a AC component which is decaying. The rate of decay depends on the voltage at the time when fault occurs and on the power factor (pf) of the system. The fault characteristics can be divided into three time categories:

- Sub-transient- which is immediately following the fault occurrence, and is associated with the largest currents.
- Transient- this is associated with the DC and AC decay of the fault current after sub-transient period.
- Steady-state- which occurs after all the transients have had time to settle and the characteristics are not changing with time.

Short-circuit analysis ensure that electrical equipment used for generation, transmission, and distribution of power is designed to interrupt SCC. Short circuits on the electrical distribution system (EDS) cannot be completely eliminated[04].

To clear fault to protect fire is the first goal for protection[03]. And second is to think about the way which reduces fault effects and to improve ….

1-Reliability is improved as coordination of devices is proper.
2-Power quality by reducing the voltage sags duration [03].

1.8.1 Standards for Fault Calculation

There are 4 main calculation methods for short circuit studies. They are as follows-

- Nodal method
- Symmetrical component method
- Complete method
- Dynamic time method

The choice of method depends on the fault type, final application and level of detail required. However, the symmetrical component and superposition methods or methods based on these are the most widely used, both for hand calculations and as well as in power system simulation tools such as DIgSILENT Power Factory, ETAP etc.

1.8.2 Overview of Standards

A number of standards are available for calculation of SCC. The most important are as explained below.

- IEC 60909-2001 - Short-circuit currents in 3-phase a.c systems. Part 0: calculation of currents.
- VDE 0102:2002-07 - Short-circuit currents in 3-phase a.c. systems - Part 0: Calculation of currents (IEC 60909-0:2001); German version EN 60909.
- IEEE 141-1993 - IEEE recommended for electric power distribution for industrial plants.
- ANSI C37.010.1999 - IEEE application guide for a.c. high-voltage circuit breaker rated on a symmetrical current basis.
- ANSI C37.5 Methods to determine the rms value of current(sinusoidal) and recovery voltage (normal frequency), and for calculating the fault currents.

1.9 LITERATURE REVIEW

[01][De Mello, Dugan and Kroposki] Explains that it is "rule of thumb" that amount of fault current contributed by distributed energy resources based on inverter is one to two times of inverter's full load current.

[02][J.Keller, B.Kroposki] Describes the characteristics of distributed energy resources based on inverter and conclude that behaviour of inverters is different as from synchronous or induction machines as rotating mass component is not their in inverters therefore they don't develop inertia which carry fault current. Inverters have a faster decaying as the devices lack inductive behaviour that are present in synchronous or induction machines.

[03][Farshid Adbolahnejad Baroogh , Milad Gheydi] calculated SCC value type-3 and type-4 wind turbines which are connected to IEEE 33-bus system using ETAP considering four scenarios as case studies. It is observed that fault contributed by Type-3 is more compared to Type-4 wind turbine.

[04][Boljevic and S.Conlon] Explains the contribution of DG on short circuit level to distribution network and also tells about various factors responsible for that.

[05][S. N. Afifi , H.Wang, G.A.Taylor] Describes the impact of DFIG penetration on SCC level of IEEE-13 network and observed that the impact of 3-ph is highest and of LG fault is lowest.

[06][Lasantha Meegahapola] Presents analysis for electrical network for high penetration of wind turbines. Rotor angle and voltage stability criteria is evaluated to

determine transient stability of system on IEEE-14 bus system at different penetration levels of wind system .

[07][S. N. Afifi and M. K. Darwish] describes the impact of hybrid renewable energy (PV and Type-3 WTG) on SCL using ETAP on 13-bus network.

[08][Muhammad Aslam] Describes that SCL of network increases with DGs interconnection as it is necessary to increase of CB capacity for reliable system operation. This type of variation in SCL depends basically upon location and type as well as size of DG.

[09] [K. A. folly , S. P. sheetekela] Compares the transient stability effect of fixed speed (SCIG) and variable speed (DFIG) wind generators connected to grid on the electrical network.

[10] [Romeu, Reginatto and Carlos Rocha] Explains the problem of determining the minimum value for the short-circuit ratio which is adequate for the interconnection of a given wind farms to a given grid point.

[11] [Elias K. Bawan] Determine the impact of DG , to reduce the power losses and to increase the voltage profile of distribution system based on location of DG and size of injection.

CHAPTER 2

BASIC DATA OF IEEE-37 BUS DISTRIBUTION NETWORK

2.1 LOAD MODELS

Loads can be spot load or assumed to be uniformly distributed load. Loads can be 1-phase or 3-phase. Three-phase loads available in delta or wye while 1-phase loads available in LN (ground) or LL connection. All electrical loads can be modelled as constant kilo watt and kilo volt ampere reactive, constant current (I) or constant impedance (Z)[29].

TABLE 2.1- NUMERIC CODES LISTS THAT WILL DESCRIBE THE LOADS.

CODE NO.	CONNECTION	MODEL
1	Wye	Const. kW, kVAr
2	Wye	Const. I
3	Wye	Const. Z
4	Delta	Const. kW, kVAr
5	Delta	Const. I
6	Delta	Const. Z

1-phase loads connected LL i.e delta will be given code numbers four, five or six. All load data is given in per phase. For cont. Z and const. I loads, the kW and kVAr given at rated voltage i.e 1.0 per unit. For wye connected loads, code no. one, two and three will be given which is connected as a-n, b-n and c-n respectively and for delta loads a-b, b-c and c-a will be used respectively. All bus loads except non-zero bus loads are assumed to be zero.

2.2CONDUCTOR DATA

TABLE 2.2- CONDUCTORS CHARACTERISTICS THAT ARE USED IN FEEDERS

CONDUCTOR	TYPE	RESISTANCE (ohm/mile)	DIAMETER (inch.)	GMR (ft.)	Amp
1000000	1	0.1050	1.1500	0.03680	698
556500	2	0.1860	0.9270	0.03110	730
500000	1	0.2060	0.8130	0.02600	483
336400	2	0.3060	0.7210	0.02440	530
4/0	2	0.5920	0.5630	0.00814	340
2/0	1	0.7690	0.4140	0.01250	230
1/0	2	1.1200	0.3980	0.00446	230
1/0	3	0.6070	0.3680	0.01113	310
#2	1	1.5400	0.2920	0.00883	156
#2	2	1.6900	0.3160	0.00418	180
#4	2	2.5500	0.2570	0.00452	140
#10	3	5.9030	0.1020	0.00331	80
#12	3	9.3750	0.0810	0.00262	75
#14	3	14.8720	0.0640	0.00208	20

1-AA , 2-ACSR , 3-CU

2.3 DATA OF LINE SECTION

Every feeder line will have a table of "Data of Line Section" and that consist of the bus terminations of each section of line (Bus A) and (Bus B), length of line and configuration code. Each system will have a "Table of Configuration Codes" that will tell about configuration code which is a unique number assigned to explain the spacing model, phasing and conductors (phase and neutral).

2.4 IEEE 37 BUS DELTA RADIBL DISTRIBUTION SYSTEM

Circuit diagram for this feeder is shown below in Figure 2.1.

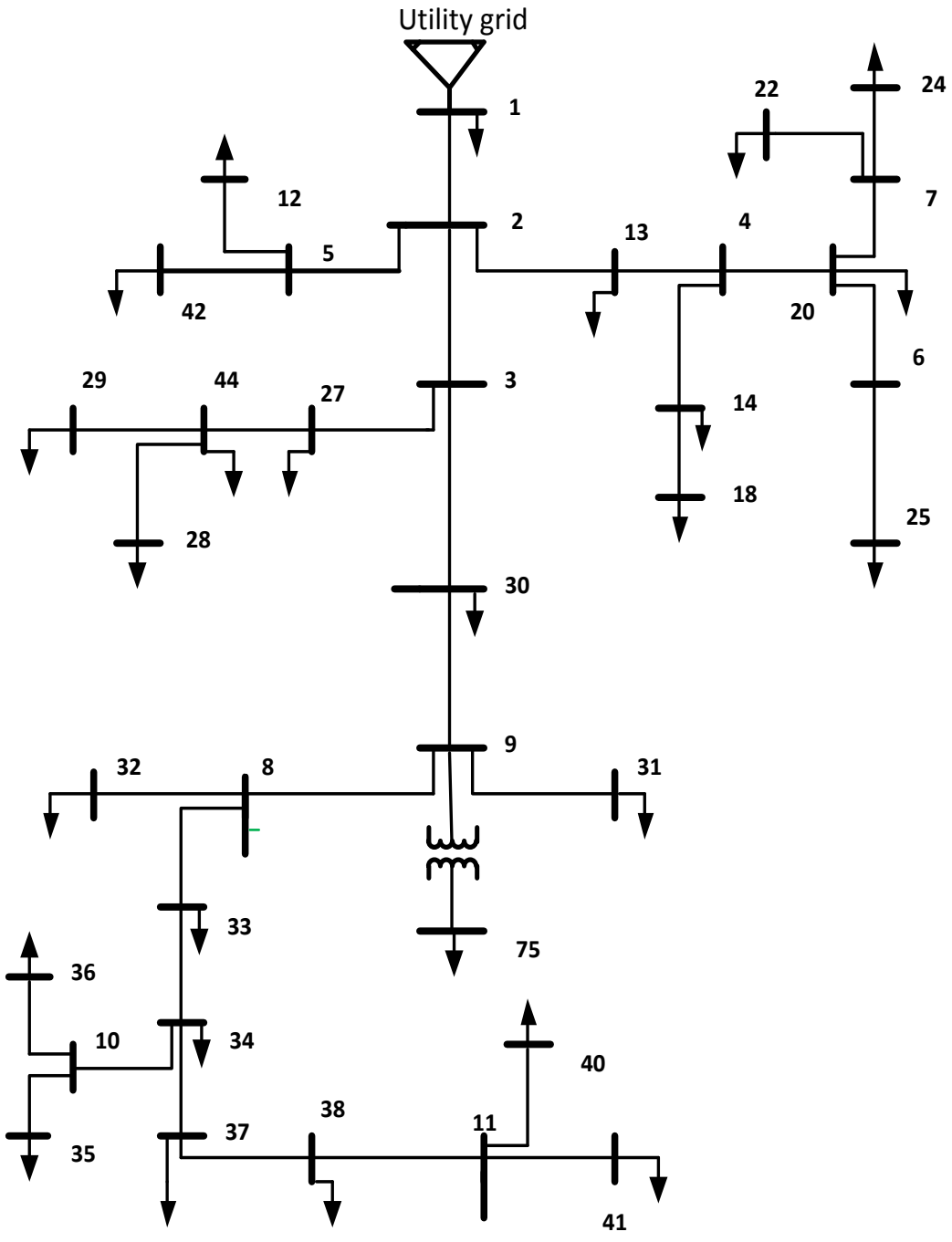

Figure 2.1- 37 Bus Delta Circuit Diagram

TABLE 2.3-IEEE **37** BUS LINE SECTION DATA

BUS A	**BUS B**	**LENGTH (FT)**	**CONFIG. CODE**
1	2	960	322
2	5	400	325
2	13	360	323
2	3	1320	322
3	27	240	325
3	30	600	323
4	14	80	325
4	20	800	323
5	42	320	325
5	12	240	325
6	25	280	325
7	24	760	325
7	22	120	325
8	33	320	323
8	32	320	325
9	31	600	323
9	8	320	323
10	35	200	325
10	36	1280	325
11	41	400	323
11	40	200	325
13	4	520	323
14	18	520	325
20	7	920	325
20	6	600	323
27	44	280	325
30	9	200	323
33	34	560	323
34	37	640	323
34	10	520	325
37	38	400	323
38	11	400	323
44	28	200	325
44	29	280	325
75	9	1	10
99	1	1850	321

TABLE 2.4-IEEE 37 BUS UNDERGROUND LINE CONFIGURATIONS

CONFIG. ID	PHASING	PHASE COND. AA	CONCENTRIC NEUTRAL COPPER	SPACING ID#
321	A B C	1000 KCM	20 - #10	321
322	A B C	500 KCM	16 - #12	322
323	A B C	2/0	7 - #14	323
325	A B C	#2	10 - #14	325

TABLE 2.5-IEEE 37 BUS UNDERGROUND LINE SPACING

SPACING ID	A-B (Inch)	B-C (Inch)	C-A (Inch)
321	2.074	2.074	2.060
322	1.603	1.603	1.570
323	1.146	1.146	1.120
325	1.030	1.030	0.970

TABLE 2.6- BUS LOADS AS KW AND KVAR

BUS NO.	LOAD MDL.	PH-1 KW	PH-1 KVAR	PH-2 KW	PH-2 KVAR	PH-3 KW	PH-3 KVAR
1	4	140.47	69.74	140.47	69.74	350.75	174.15
12	4	0.00	0.00	0.00	0.00	84.11	41.76
13	4	0.00	0.00	0.00	0.00	84.11	41.76
14	5	16.82	8.35	21.03	10.44	0.00	0.00
18	6	84.11	41.76	0.00	0.00	0.00	0.00
20	4	0.00	0.00	0.00	0.00	84.11	41.76
22	5	0.00	0.00	140.47	69.74	21.03	10.44
24	6	0.00	0.00	42.06	20.88	0.00	0.00
25	4	0.00	0.00	42.06	20.88	0.00	0.00
27	4	0.00	0.00	0.00	0.00	42.06	20.88
28	4	42.06	20.88	42.06	20.88	42.06	20.88
29	5	42.06	20.88	0.00	0.00	0.00	0.00
30	6	0.00	0.00	0.00	0.00	84.11	41.76
31	6	0.00	0.00	84.11	41.76	0.00	0.00
32	4	0.00	0.00	0.00	0.00	42.06	20.88
33	5	84.11	41.76	0.00	0.00	0.00	0.00
34	4	0.00	0.00	0.00	0.00	42.06	20.88
35	4	0.00	0.00	0.00	0.00	84.11	41.76
36	6	0.00	0.00	42.06	20.88	0.00	0.00
37	5	140.47	69.74	0.00	0.00	0.00	0.00
38	4	126.17	62.64	0.00	0.00	0.00	0.00
40	4	0.00	0.00	0.00	0.00	84.11	41.76
41	5	0.00	0.00	0.00	0.00	42.06	20.88
42	6	8.41	4.18	84.11	41.76	0.00	0.00
44	4	42.06	20.88	0.00	0.00	0.00	0.00
TOTAL	**……..**	**726.74**	**360.81**	**638.43**	**316.96**	**1086.74**	**539.55**

2.5- ETAP IEEE 37-BUS TEST SYSTEM

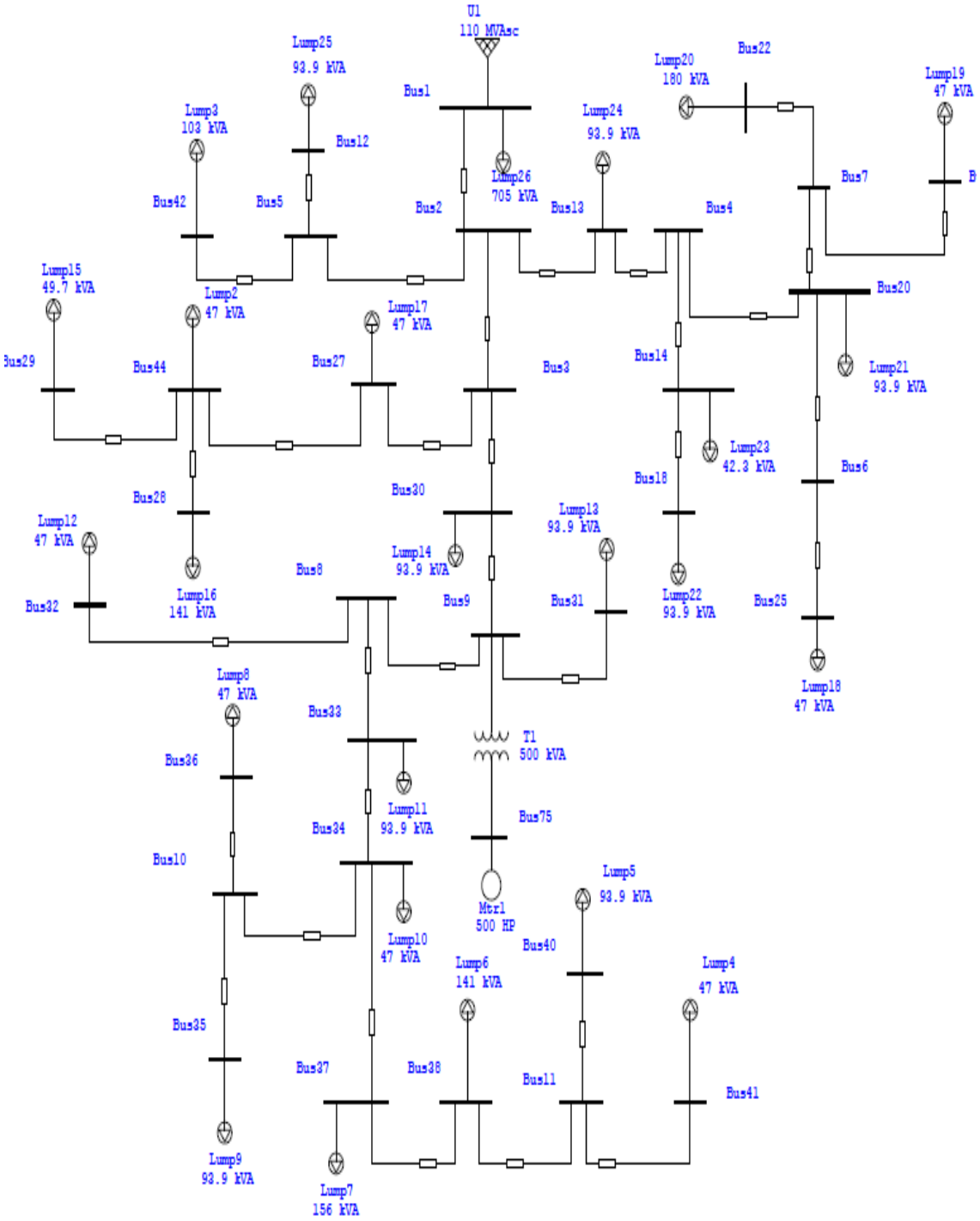

Figure 2.2- IEEE 37-Bus Distribution Test System Model

2.6- LOAD FLOW RESULT OF IEEE 37-BUS SYSTEM

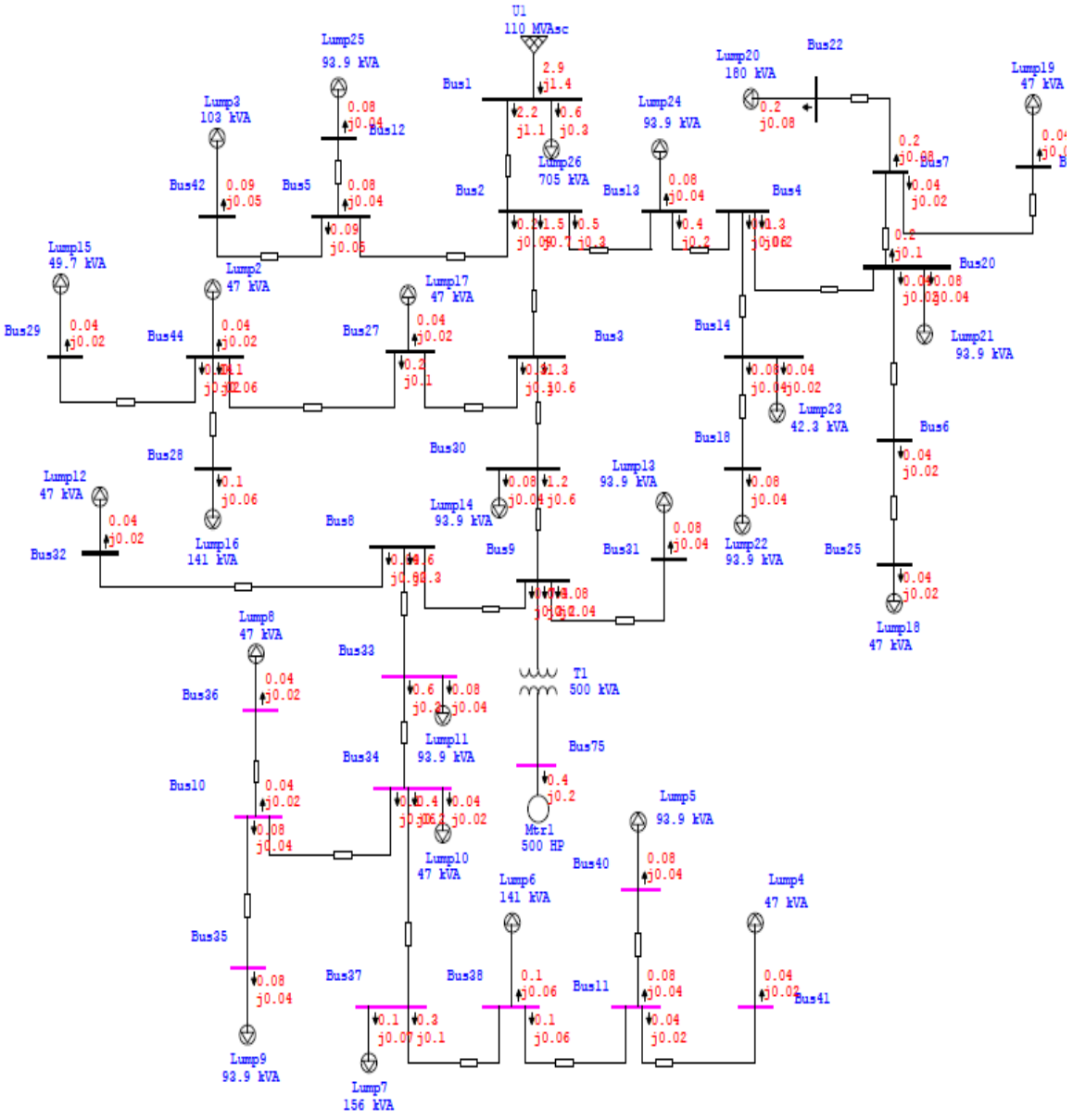

Figure 2.3- Load Flow Result Indicating MW and MVAR

CHAPTER 3

IMPACT OF DFIG ON SHORT CIRCUIT LEVELS

3.1 INTRODUCTION

The number of DGs interconnection to grid is increasing day by day. The behaviour of turbine connected to grid system has been investigated[17]–[20].But the contribution of DG like WTG to short circuit level (SCL) is not getting attention. The SCC effect is important for network protection, and to know maximum currents allowed in a power network [21], [22].

In a variable-speed turbines with a PEC between stator and grid, the SCC can be estimated comparatively easily, which generally not more than the nominal current of the converter [23].Wind turbines like constant-speed and a variable-speed turbine with DFIG, both have grid connected induction machine. The SCC behaviour of induction machines is depends on characteristics of machine[23]. A DFIG is directly grid coupled and it also have PEC between rotor and grid. Voltage drop will cause large, oscillatory currents in the stator windings. Due to coupling between stator and rotor, current will pass to rotor and through the PEC.

The DG may introduce various advantages such as.

- Unloading sub-transmission and transmission system.
- Decreasing losses.
- Enhancing reliability and power quality.

In this thesis, the impact of DFIG turbines on SCL of 37-bus test system by ETAP 12.6 software is examined which includes various types of faults such LLLG, SLG, LL, and LLG. Here comparison of SCL for different fault types for different scenarios is presented and discussed.

3.2 DOUBLY FED INDUCTION GENERATORS

The DFIG is basically a WRIG in which the rotor circuit is controlled by power electronics devices for getting variable speed. A block diagram of the DFIG is shown below in Figure 3.1and its mathematical modeling for SCC calculation is explained in APPENDIX A.

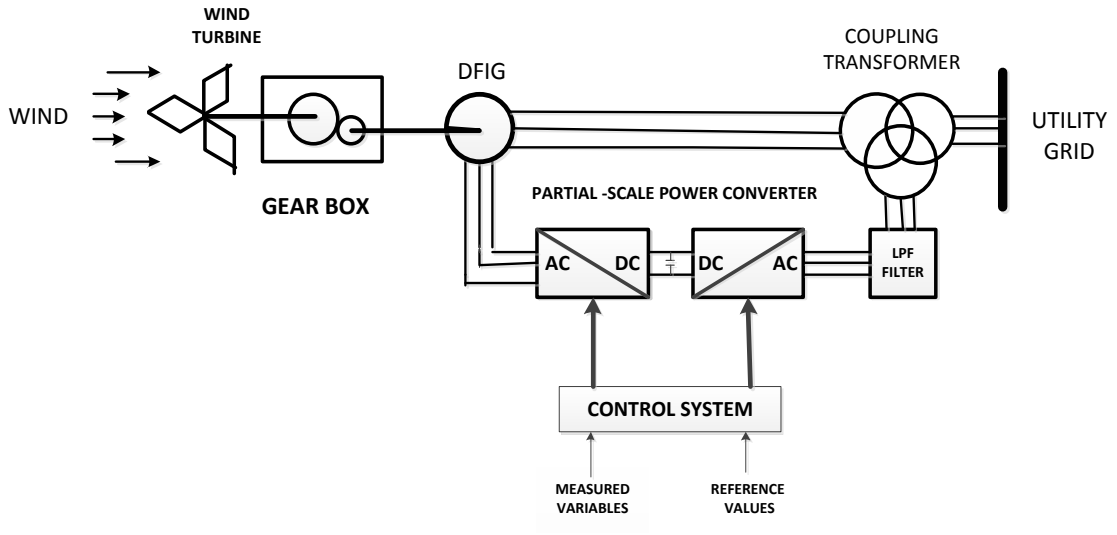

Figure 3.1- Block Diagram of the DFIG Turbine

3-phase a.c windings of stator and rotor that provides speed around ±30% of synchronous speed [14].The three phase stator winding is directly connected to grid through a transformer, whereas the three phase rotor windings are connected to grid through RSC, GSC and filters[15]. Active power flow from stator is unidirectional. However, it is bidirectional when flows rotor to grid depending upon mode of operation .The power rating of converter which depends range of speed of operation is around 30% of the nominal rated power output of turbine [14]. General data of TYPE-3 generic wind turbine used for fault current calculation in 37 bus distribution network are- Nominal power: 1,000 kW, Rotor diameter: 60m, Swept area: 2828m^2, Air Density = 1.225 kg/m3, Power control: Pitch, Start-up wind speed: 4 m/s, Nominal wind speed: 15 m/s and Maximum wind speed: 25 m/s. Average wind speed for performing experiment is taken as 16 m/s. Its curves like power curve, wind profile curve and wind power coefficient curve of 1 MW type -3 DFIG is shown below

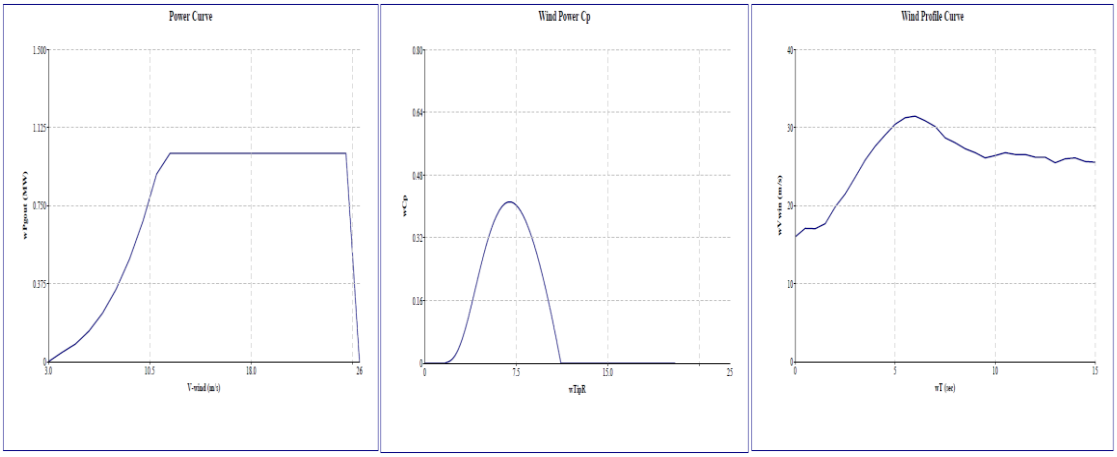

Figure 3.2-Power, Wind Profile and Power Coefficient Curve

3.3 **SYSTEM UNDER STUDY**

The short circuit analysis is performed on 37-bus test system using the ETAP12.6 software. Line diagram of the simulated system is shown below in Figure 3.3.

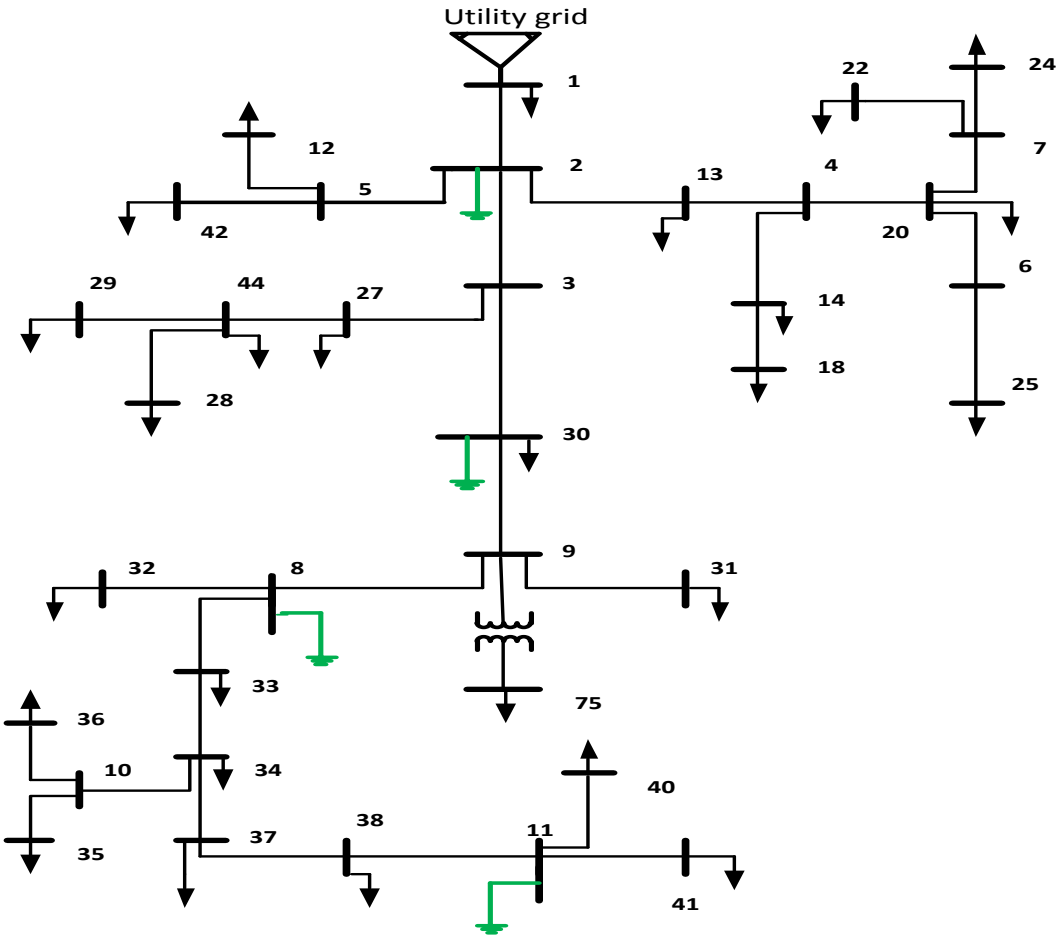

Figure 3.3- IEEE-37 Bus Distribution System

Six scenarios are created here to determine impact of Type-3 WTG on SCL on IEEE-37 bus network is given in Table 3.1. Scenarios are varied to obtain reliable and valid results. Simulation examine the occurrence of different types of fault (3-ph, SLG, LL, LLG) at different buses 2,30,8,11 respectively. The criterion of buses selection where based on distance from the main grid and loads concentration. Then results are analysed based on comparing SCL values at each six different scenario with no DG.

TABLE 3.1- SIX DIFFERENT SCENARIOS APPLIED FOR TYPE-3 WTG

SCENARIO	CONDITION
Scenario 1 (S1)	No DG penetration
Scenario 2 (S2)	1 MW Type-3 WTG placed at Bus-2
Scenario 3 (S3)	1 MW Type-3 WTG placed at Bus-30
Scenario 4 (S4)	1 MW Type-3 WTG placed at Bus-8
Scenario 5 (S5)	1 MW Type-3 WTG placed at Bus-11
Scenario 6 (S6)	2*0.5 MW Type-3 WTG placed at Bus-8 and 30

3.4 SIMULATED RESULT AND DISCUSSION

TABLE 3.2- SIMULATED SCC VALUES FOR TYPE-3 WTG IN (KA)

LOCATION OF FAULT	3 PHASE FAULT					
	S1	S2	S3	S4	S5	S6
BUS 2	11.832	12.431	12.410	12.405	12.383	12.123
BUS 30	7.832	8.086	8.369	8.370	8.369	8.101
BUS 8	6.686	6.865	7.098	7.190	7.198	6.915
BUS 11	3.825	3.876	3.963	4.009	4.240	3.907

LOCATION OF FAULT	LINE TO GROUND FAULT					
	S1	**S2**	**S3**	**S4**	**S5**	**S6**
BUS 2	4.099	4.155	4.153	4.152	4.149	4.136
BUS 30	2.272	2.289	2.301	2.302	2.302	2.293
BUS 8	2.000	2.013	2.024	2.026	2.028	2.018
BUS 11	1.298	1.304	1.309	1.310	1.313	1.307

LOCATION OF FAULT	LINE TO LINE FAULT					
	S1	**S2**	**S3**	**S4**	**S5**	**S6**
BUS 2	10.309	10.955	10.926	10.918	10.886	10.736
BUS 30	6.843	7.116	7.427	7.428	7.422	7.254
BUS 8	5.841	6.031	6.285	6.390	6.396	6.190
BUS 11	3.330	3.382	3.476	3.526	3.787	3.449

LOCATION OF FAULT	DOUBLE LINE TO GROUND FAULT					
	S1	**S2**	**S3**	**S4**	**S5**	**S6**
BUS 2	10.459	11.108	11.072	11.062	11.022	10.872
BUS 30	7.050	7.322	7.595	7.599	7.601	7.426
BUS 8	6.079	6.272	6.502	6.585	6.600	6.398
BUS 11	3.563	3.618	3.706	3.750	3.968	3.675

The amount of fault contributed by different type of DG is determined by factors [13] such as:

- The type of DG used, as different types will contribute different amount of fault currents.
- The distance from the point of fault, as the increased line impedance will reduce the amount of fault current.
- Presence of transformer as its short circuit impedance may limit the fault current.
- Network configuration between DG and fault, as for different paths fault current magnitude will be different.

- Method of coupling of DG to network as directly connected system will contribute higher currents as compared to via PEC [1].

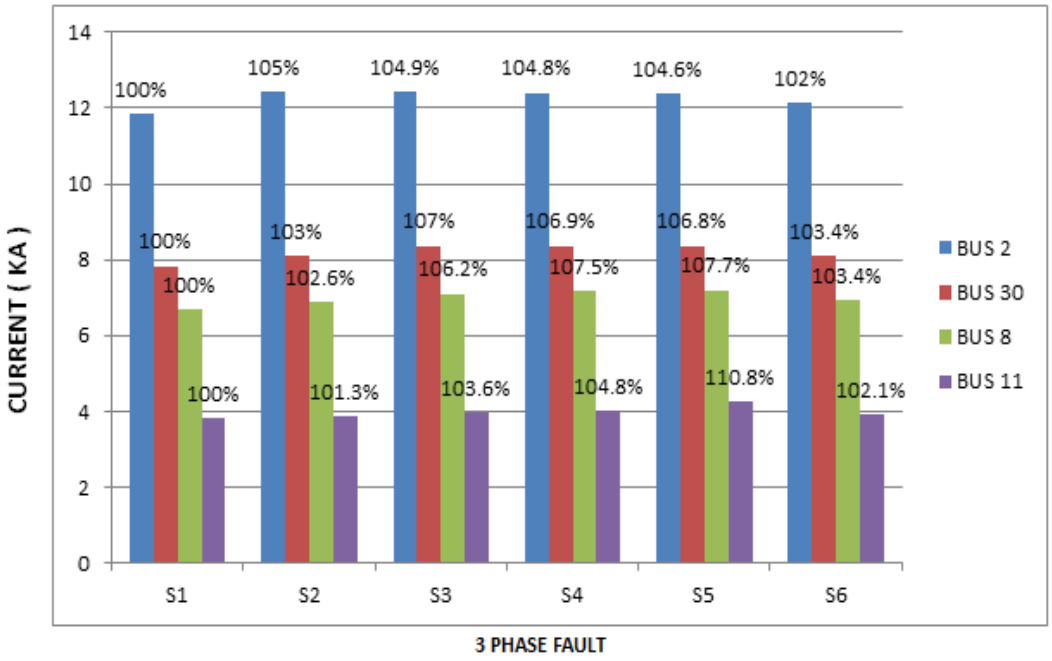

Figure 3.4- SCC in Different Scenarios for Three Phase Faults in Case of Type-3 WTG.

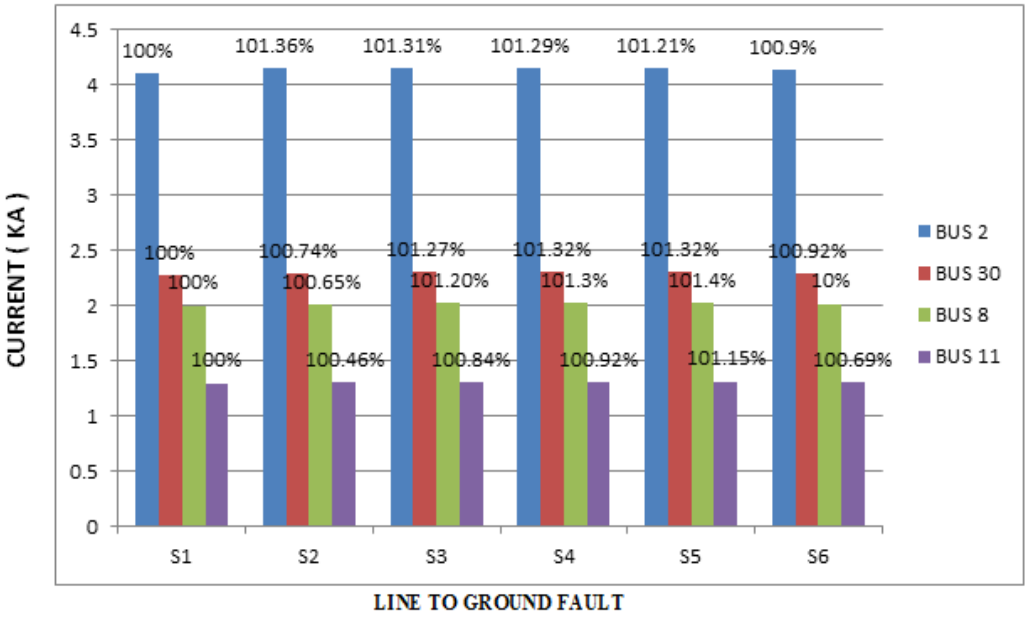

Figure 3.5-SCC in Different Scenarios for SLG Fault in Case of Type-3 WTG

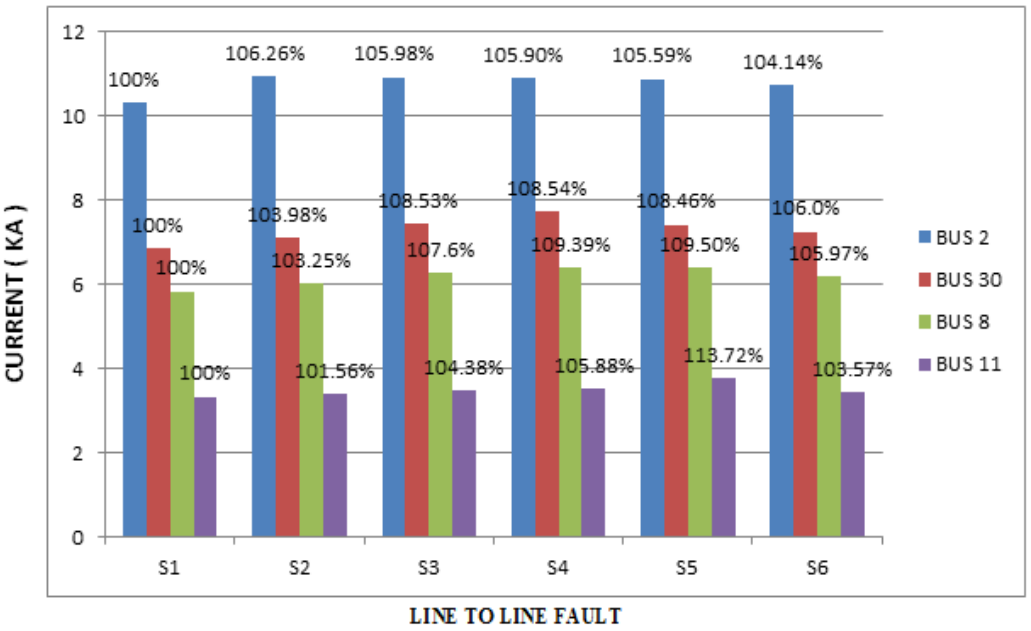

Figure 3.6 SCC in Different Scenarios for LL Faults in Case of Type-3 WTG

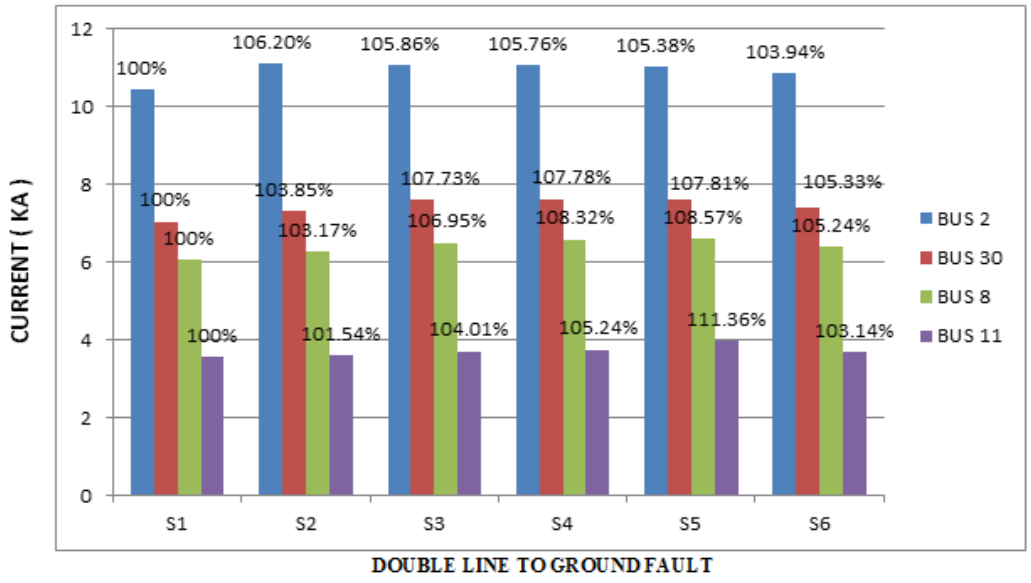

Figure 3.7- SCC in Different Scenarios for LLG Faults in Case of Type-3 WTG

In this chapter, the impact of different location and size of Type-3 WTG on SCL of IEEE-37 bus distribution system by ETAP 12.6 software is given. Here results are obtained by using ETAP (ANSI standard, C37.010-1999) which is capable of calculating rms values

of current at 1/2 cycle (maximum short circuit current), rms value of current during 1.5 to 4 cycle and rms values at 30 cycles (minimum short circuit current).
All results shown in this thesis are rms values of fault current during 1.5 to 4 cycles. Here results are shown for all four types of faults as shown in table 3.2 for six different scenarios. The impact of various types of fault on the SCL in all scenarios applied follows a sequence 3- phase fault, LLG fault, LL and SLG. That is it shows highest impact for 3-ph and least impact for LG fault.

It is also observed from bar graph that change in the SCL level is huge (around 3-9 %) for scenarios 2 to 6 (WTG Type-3 connected) in comparison with scenario 1(without WTG power plant). Figure 3.4-3.7 shows comparisons of fault currents taking WTG power plant location and the type of fault as a percentage of without WTG. From above figures it could be noticed that when fault occurs at node 2 (near utility grid), the short circuit current is so significant (even greater than PV and HYBRID as discussed in chapter 4 and 5) compared with the SCC for all types of fault and scenarios if a fault occurs at nodes 8, 11 or 30. At scenarios 3, 4 and 5 the SCC has the highest values when a fault occurs at node 30, 8 and 11 respectively and a 1MW Type-3 WTG power plant is located at the same bus.

3.5 CONCLUSION

In this chapter the effect of DFIG penetration on the SCL of IEEE 37-bus distribution network by comparing six different scenarios by varying location of the WTG is analysed. The three-phase type fault had the severe impact followed by double line to ground followed by line to line fault. Conversely, the line to ground (SLG) fault represented the lowest impact. The highest SCL always observed at bus (near the grid) for six different locations of DFIG for various types of fault. Conversely, lowest occurred at the farther bus with respect to grid in the six different scenarios for various types of fault. This behaviour of Type-3 WTG is because of its connection with the grid (stator directly coupled and rotor is coupled by PEC) [02].

CHAPTER 4

IMPACT OF PV SYSTEM ON SHORT CIRCUIT CURRENT LEVELS

4.1 INTRODUCTION

DG is basically stated as generators (up to 250-300 MW) that provide 'P', connected directly to the power system network. Common types of DG are shown in figure 4.1 The DG like PV is proved to be an excellent solution to various obstacles. Rapid growth of PV networks demands intensive analysis to determine its impact. The short-circuit is one of the important factors causing transients in network which affect the fault clearing time and relaying interference. The main reason of DG interconnection to system is that, the SCL at PCC,will not exceed the designed value.

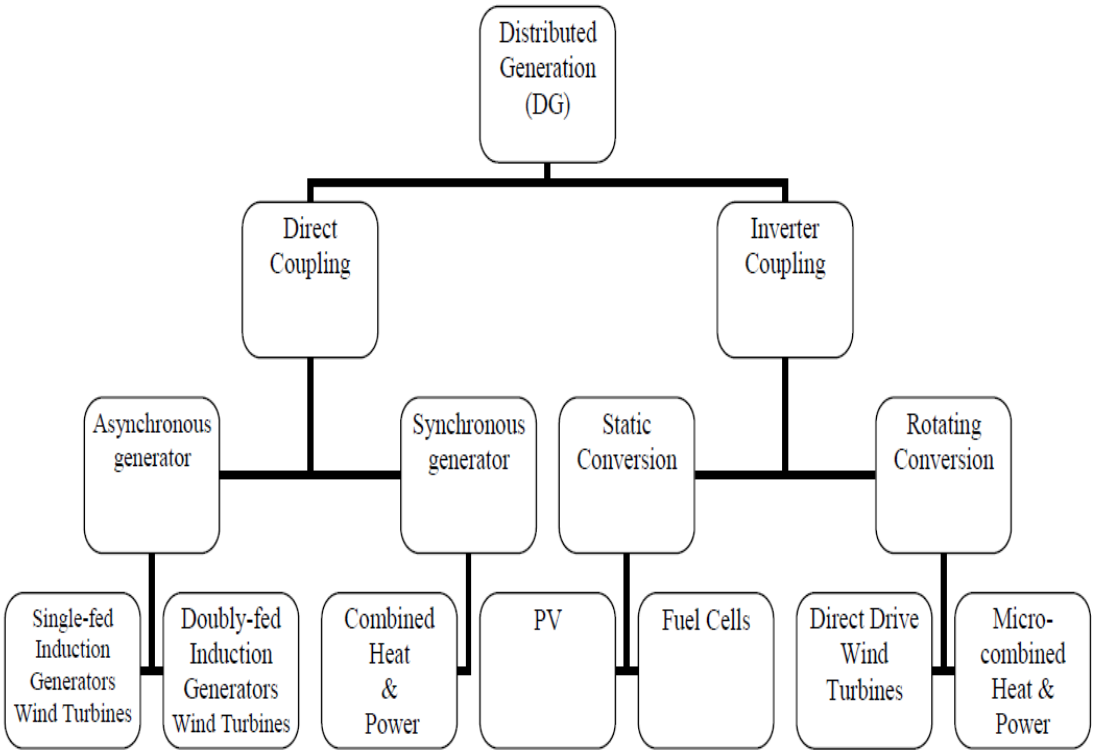

Figure 4.1- Classification of DG

4.2-PHOTOVOLTAIC POWER SYSTEM

The pv represents fastest growing source of energy(renewable) worldwide. By 'Photovoltaic effect' we can directly convert sunlight into energy (electrical) which occur by photovoltaic cell. By grouping PV cells module is formed. And therefore number of modules are connected in a series-parallel configuration to produce the required amount of power. Array output power is affected by conditions such as location, irradiance, and temperature as explained in chapter 1. Figure 4.2 shows a basic PV system .The PV modules are connected via inverters, to convert the DC into AC power.

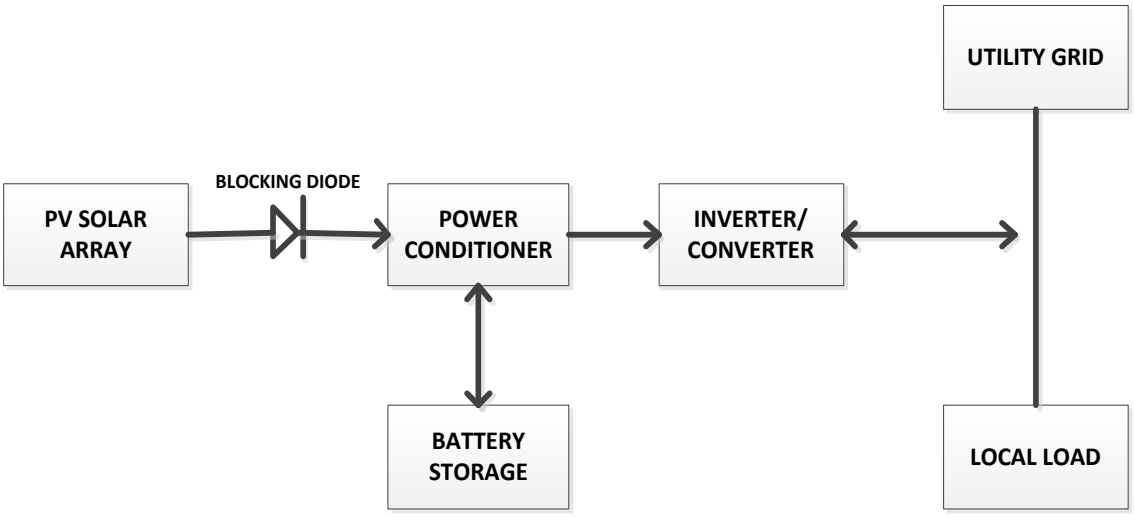

Figure 4.2- Block Diagram of PV System

4.3 SYSTEM UNDER STUDY

In this chapter impact of 1MW PV source on SCL on IEEE 37-bus system has been examined using Etap12.6 software as a tool for simulation. Line diagram of the system under consideration is shown in chapter 3 (Figure 3.3). Six different scenarios are examined as shown below in table 4.1.

TABLE 4.1- SIX DIFFERENT SCENARIOS APPLIED

SCENARIO	CONDITION
Scenario 1 (S1)	No DG penetration
Scenario 2 (S2)	1 MW PV farm placed at Bus-2
Scenario 3 (S3)	1 MW PV farm placed at Bus-30
Scenario 4 (S4)	1 MW PV farm placed at Bus-8
Scenario 5 (S5)	1 MW PV farm placed at Bus-11
Scenario 6 (S6)	2*0.5 MW PV farm placed at Bus-8 and 30

The simulation examine different fault (3-ph, LG, LL,LLG) at buses 2,30,8,11 respectively. Selection criterion of buses is distance from the main grid and the loads concentration. Then results are analysed by comparing the SCL values at different scenario with and without DG interconnection. The specifications of single PV array used for generating 1MW power by connecting no. of array in series and parallel are as given below:

Short-circuit current, I_{SC} = 7.470 A,
Open circuit voltage, V_{OC} = 21.970 V,
Maximum power, P_{MAX} = 120.30 W,
Current for maximum power, I_{MP} = 6.910 A,
Voltage for maximum power, V_{MP} = 17.410 V, and
Solar Irradiance is = 1000 W/m2.

4.4 RESULTS AND DISCUSSION

TABLE 4.2- SIMULATED SCC VALUES FOR 1MW PV IN (KA)

LOCATION OF FAULT	3 PHASE FAULT					
	S1	**S2**	**S3**	**S4**	**S5**	**S6**
BUS 2	11.832	11.853	11.850	11.849	11.846	11.868
BUS 30	7.832	7.839	7.875	7.874	7.871	7.971
BUS 8	6.686	6.691	6.711	6.737	6.734	6.762
BUS 11	3.825	3.827	3.828	3.835	3.890	3.838

LOCATION OF FAULT	LINE TO GROUND FAULT					
	S1	**S2**	**S3**	**S4**	**S5**	**S6**
BUS 2	4.099	4.100	4.100	4.099	4.099	4.101
BUS 30	2.272	2.272	2.275	2.275	2.275	2.278
BUS 8	2.000	2.000	2.002	2.004	2.004	2.006
BUS 11	1.298	1.299	1.299	1.300	1.305	1.301

LOCATION OF FAULT	LINE TO LINE FAULT					
	S1	**S2**	**S3**	**S4**	**S5**	**S6**
BUS 2	10.309	10.327	10.324	10.323	10.321	10.339
BUS 30	6.843	6.851	6.881	6.879	6.877	6.917
BUS 8	5.841	5.847	5.862	5.885	5.882	5.906
BUS 11	3.330	3.331	3.332	3.338	3.386	3.341

LOCATION OF FAULT	DOUBLE LINE TO GROUND FAULT					
	S1	**S2**	**S3**	**S4**	**S5**	**S6**
BUS 2	10.459	10.470	10.467	10.466	10.464	10.475
BUS 30	7.050	7.050	7.092	7.091	7.088	7.134
BUS 8	6.079	6.099	6.105	6.128	6.125	6.153
BUS 11	3.563	3.564	3.566	3.573	3.623	3.577

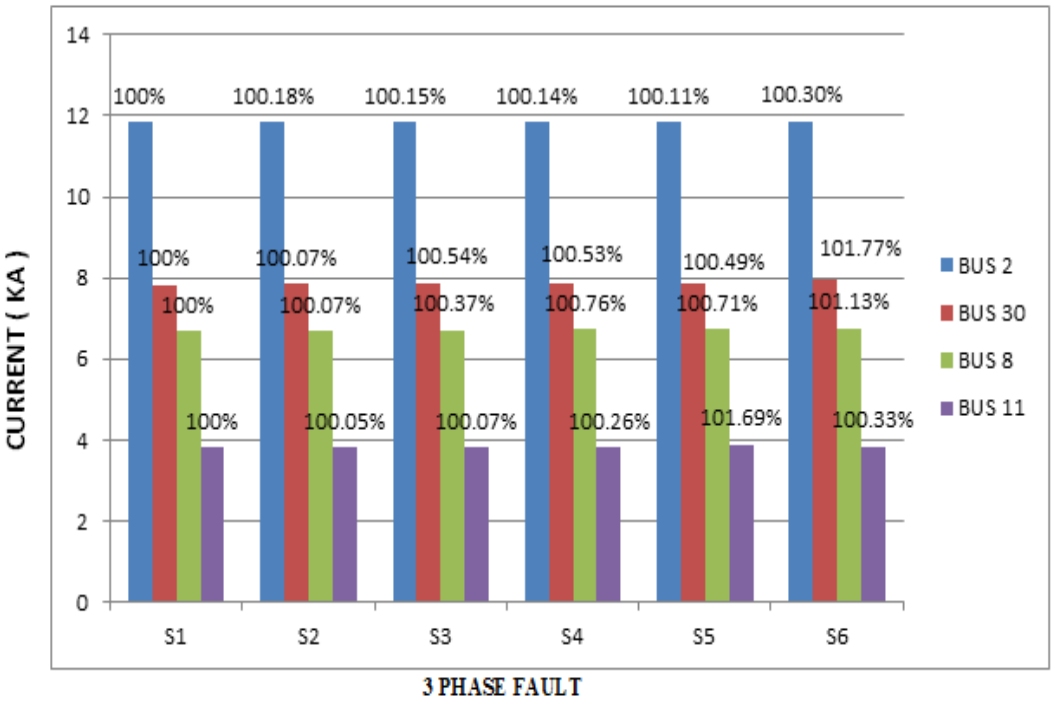

Figure 4.3- SCC in Different Scenarios for 3-Ph Fault in Case of PV

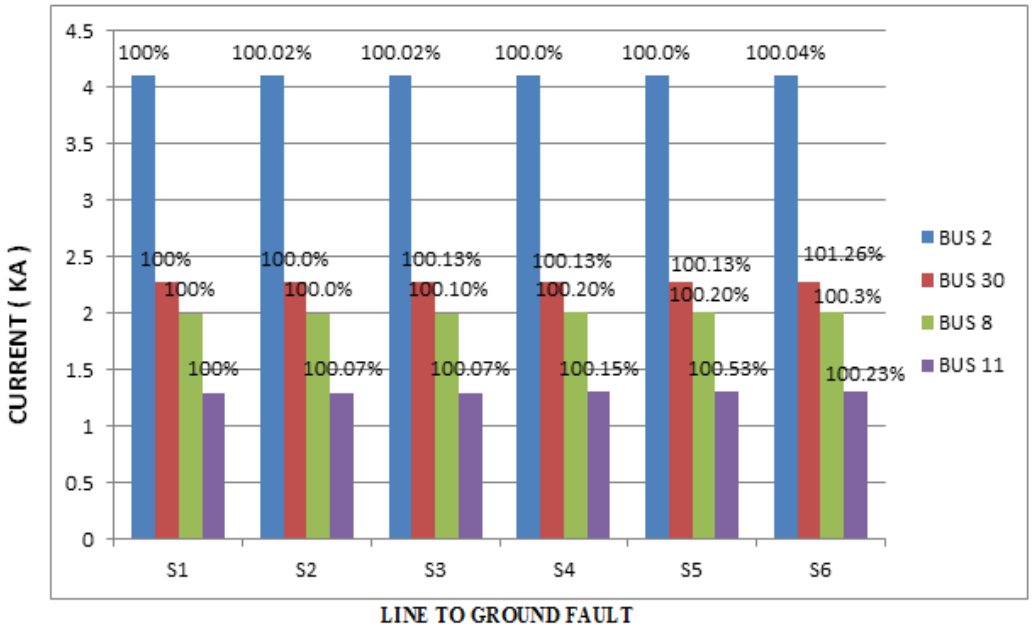

Figure 4.4- SCC in Different Scenarios for SLG Faults in Case of PV

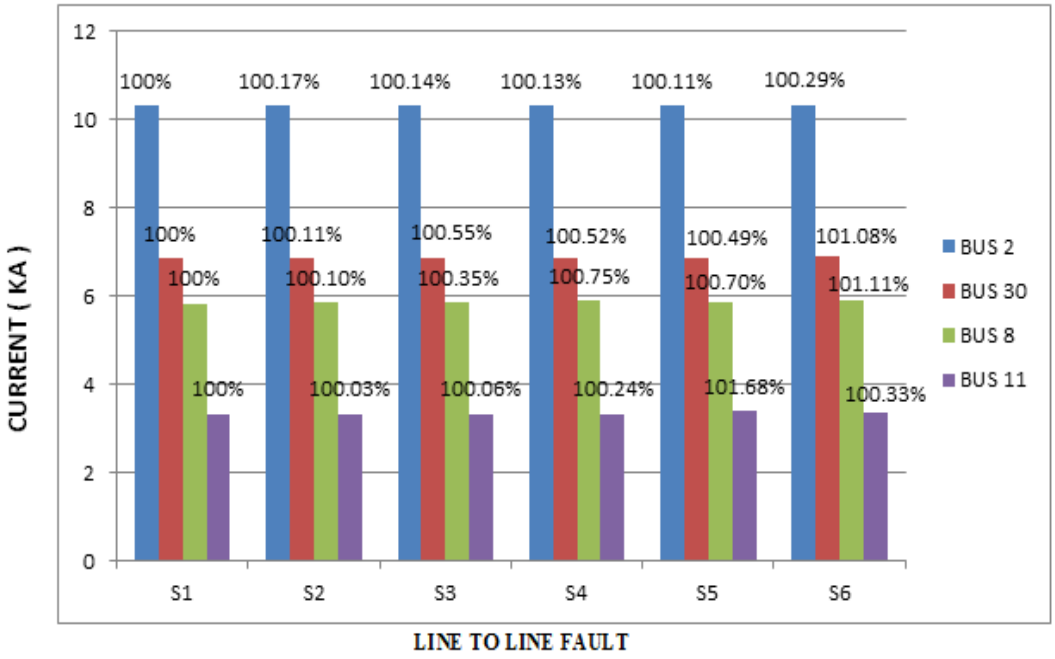

Figure 4.5- SCC in Different Scenarios for LL Faults in Case of PV

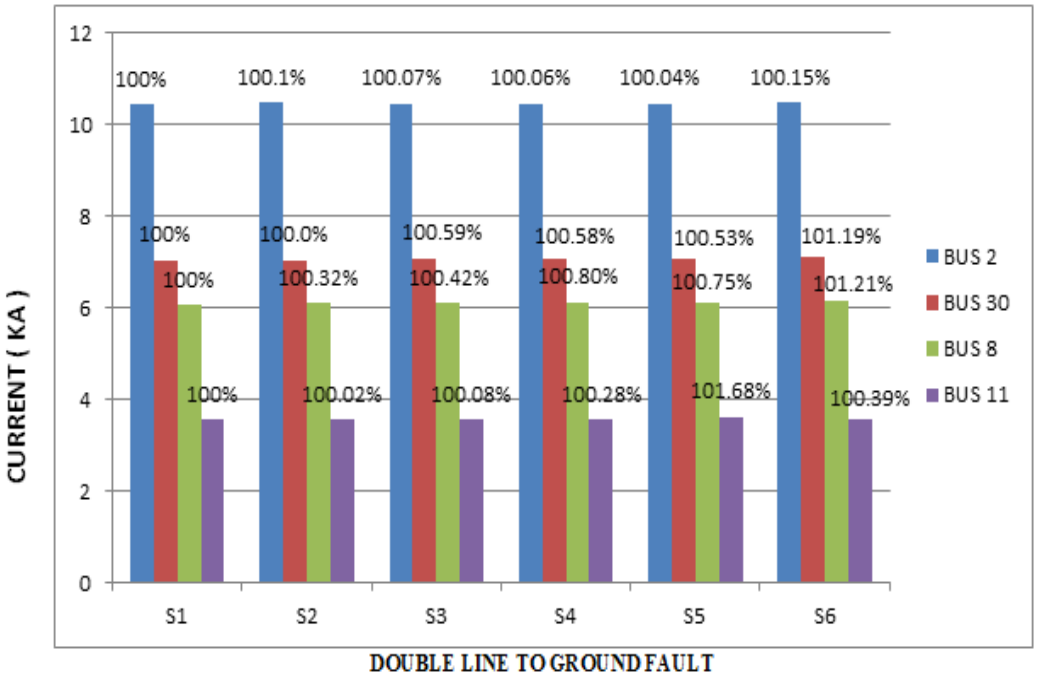

Figure 4.6-SCC in Different Scenarios for LLG Faults in case of PV

The amount of fault contributed by different type of DG is depends on no. of factors which is explained in chapter 3. Here results are obtained by using ETAP (ANSI standard, C37.010-1999) which is calculating rms values of fault current during 1.5 to 4 cycles as shown in table 4.2. The simulation results for the short circuit current analysis examining the different types of fault for the six different situations when 1MW PV is connected to distribution network are shown in Table 4.2. The impact of different types of fault on the short circuit level in all scenarios applied follows the same sequence as in case of WTG. It is also observed from bar graph that the change in the SCL is very little (around 0.2-2 %) for scenarios 2 to 6 in comparison with scenario 1. Figure 4.2-4.6 shows comparisons of fault currents taking into consideration the PV and without PV. From above results it is observed that fault level is high when fault occurs at node 2 as compared to fault at nodes 8, 11 or 30.

4.5 CONCLUSION

In this chapter, the amount of fault current contributed by grid-connected PV plant is discussed. Above simulation results confirmed that for even large PV power plant fault contributed by it is insignificant but behaviour of fault is similar to as observed in case of Type-3 WTG. This insignificant contribution is because of current limitation of inverter circuit, as it is assumed as a “rule of thumb” that total fault current contributed by inverter based DG can be of one to two times an inverter’s full load current[1],[5],[11] and explained in APPENDIX-B.

CHAPTER 5

IMPACT OF HYBRID SYSTEM ON SHORT CIRCUIT LEVELS

5.1 INTRODUCTION

Research is still going on to study the impact of renewable energy sources on the electrical power systems. Electrical power systems have three major consequential pillars generation, transmission, and distribution. This thesis is specifically concerned with the electrical distribution networks, and the effect of DG on the fault level. Major factors affecting the power distribution planning are penetration level, DG capacity, short circuit level etc. when it comes to DG integration .

5.2 SYSTEM UNDER STUDY

Here short-circuit analysis is done on IEEE 37-bus distribution test system by ETAP software as a tool. The line diagram is shown in chapter 3 in Figure 3.3. Six conditions are examined in regards to the location of Hybrid (PV and Type-3 WTG) DG from the main grid and bus loading as shown in table 5.1.

TABLE 5.1- SIX DIFFERENT SCENARIOS APPLIED FOR HYBRID

SCENARIO	CONDITION
Scenario 1 (S1)	No DG penetration
Scenario 2 (S2)	0.5 MW PV farm and 0.5MW Type-3 WTG placed at Bus-2
Scenario 3 (S3)	0.5 MW PV farm and 0.5MW Type-3 WTG placed at Bus-30
Scenario 4 (S4)	0.5 MW PV farm and 0.5MW Type-3 WTG placed at Bus-8
Scenario 5 (S5)	0.5 MW PV farm and 0.5MW Type-3 WTG placed at Bus-11
Scenario 6 (S6)	0.5 MW PV farm and 0.5MW Type-3 WTG placed at Bus-8 and 30

The specifications and rated capacity of the single PV array used for generating 0.5MW power by connecting no. of array in series and parallel are as follows:

Short-circuit current, I_{SC} = 7.470 A,

Open circuit voltage, V_{OC} = 21.970 V,

Maximum power, P_{MAX} = 120.30 W,

Current for maximum power, I_{MP} = 6.91) A,

Voltage for maximum power, V_{MP} = 17.410 V, and

Solar Irradiance = 1000 W/m2

General data of Type-3 wind turbine used are Nominal power: 500 kW, Rotor diameter: 60m, Swept area: 2828m,²Air Density : 1.225 kg/m3,Power control: Pitch, Start-up wind speed: 4 m/s, Nominal wind speed: 15 m/s and Maximum wind speed: 25 m/s. Its curves like power curve, wind profile curve and wind power coefficient curve are shown below in figure 5.1.

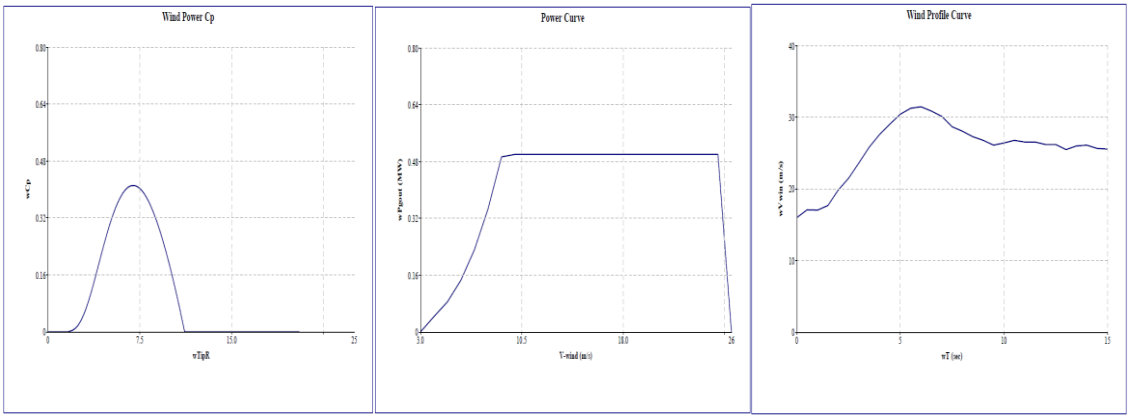

Figure 5.1- Power, Wind Profile and Power Coefficient Curve for Hybrid Case

5.3 RESULTS AND DISCUSSION

TABLE 5.2- SIMULATED SCC VALUES FOR HYBRID SYSTEM IN (KA)

LOCATION OF FAULT	3 PHASE FAULT					
	S1	S2	S3	S4	S5	S6
BUS 2	11.832	12.003	11.995	11.992	11.985	11.994
BUS 30	7.832	7.894	8.008	8.007	8.001	8.007
BUS 8	6.686	6.727	6.813	6.861	6.857	6.840
BUS 11	3.825	3.834	3.863	3.881	3.989	3.870

LOCATION OF FAULT	LINE TO GROUND FAULT					
	S1	S2	S3	S4	S5	S6
BUS 2	4.099	4.120	4.119	4.119	4.117	4.119
BUS 30	2.272	2.278	2.286	2.286	2.285	2.286
BUS 8	2.000	2.005	2.011	2.013	2.013	2.013
BUS 11	1.298	1.300	1.303	1.304	1.309	1.304

LOCATION OF FAULT	LINE TO LINE FAULT					
	S1	S2	S3	S4	S5	S6
BUS 2	10.309	10.553	10.539	10.535	10.523	10.538
BUS 30	6.843	6.936	7.085	7.083	7.075	7.084
BUS 8	5.841	5.903	6.017	6.077	6.071	6.040
BUS 11	3.330	3.345	3.383	3.407	3.544	3.389

LOCATION OF FAULT	DOUBLE LINE TO GROUND FAULT					
	S1	S2	S3	S4	S5	S6
BUS 2	10.459	10.691	10.676	10.672	10.658	10.675
BUS 30	7.050	7.144	7.278	7.277	7.271	7.277
BUS 8	6.079	6.143	6.248	6.300	6.296	6.272
BUS 11	3.563	3.579	3.615	3.636	3.756	3.622

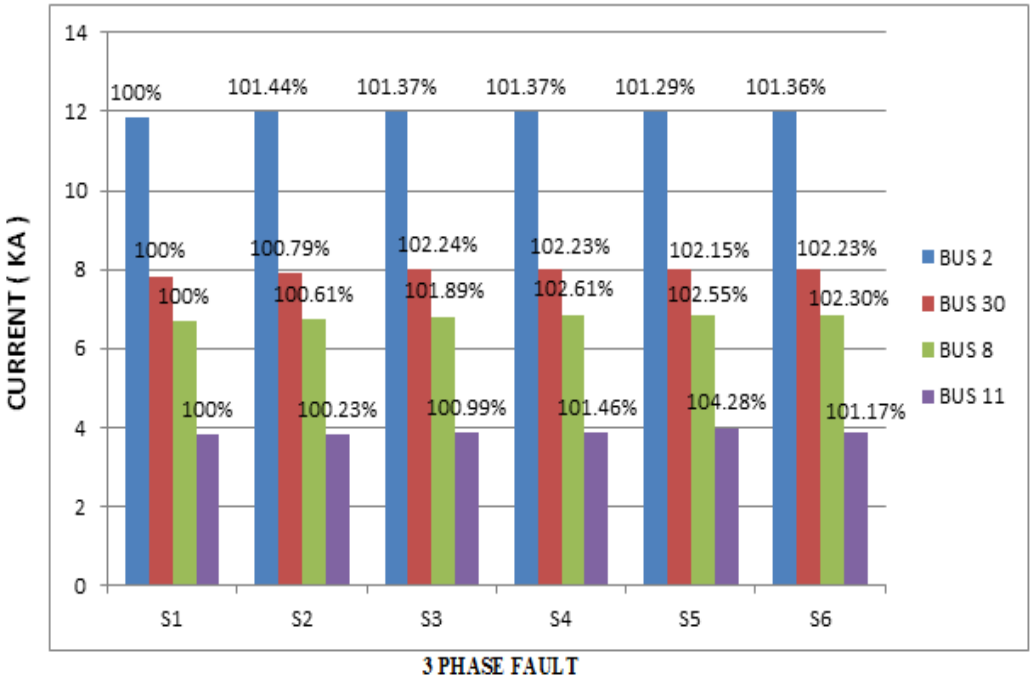

Figure 5.2- SCC in Different Scenarios for 3-Ph Faults in Case of Hybrid

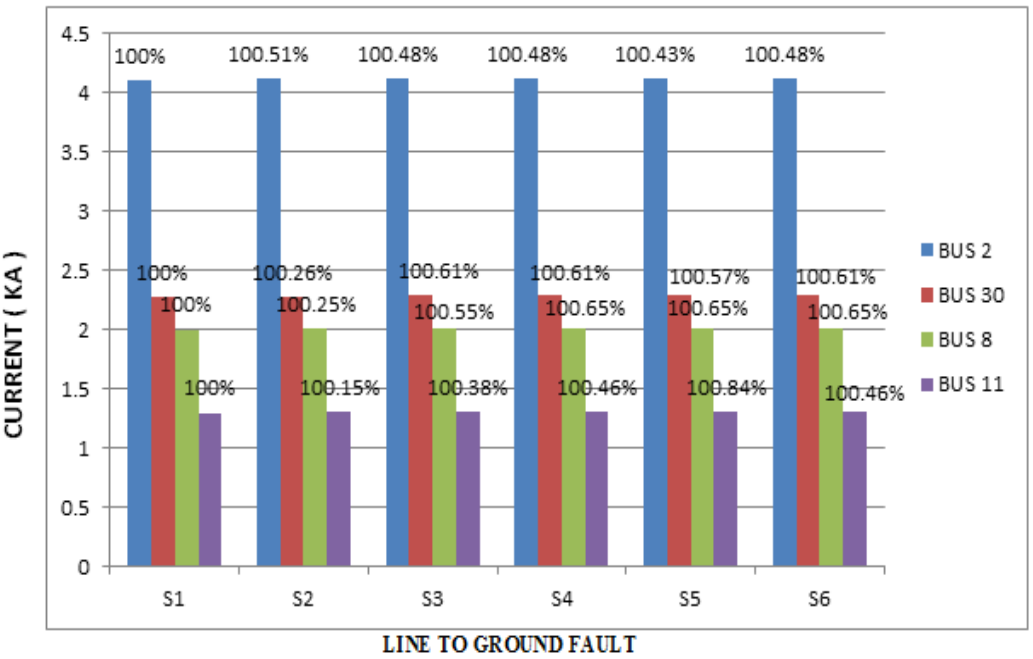

Figure 5.3-SCC in Different Scenarios for LG Faults in Case of Hybrid

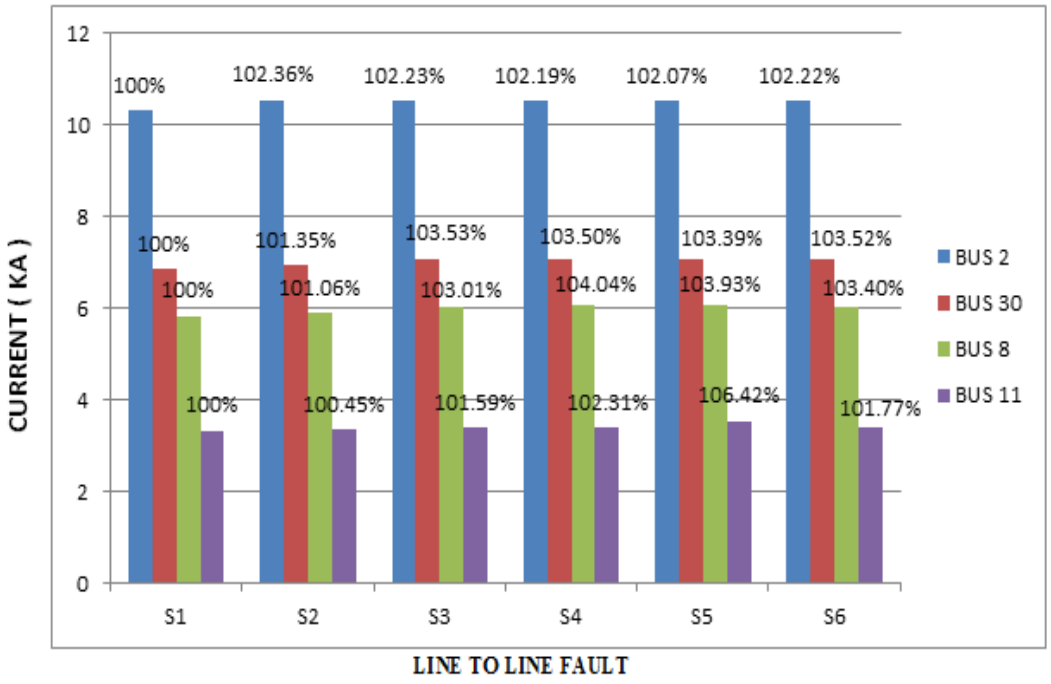

Figure 5.4-SCC in Different Scenarios for LL Faults in Case of Hybrid

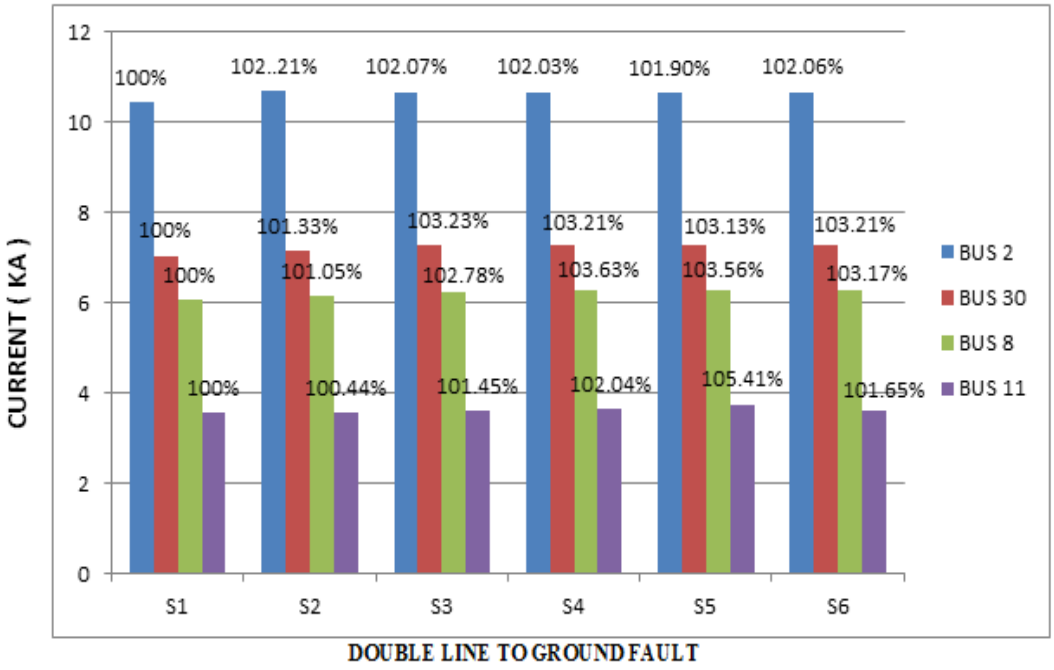

Figure 5.5- SCC in Different Scenarios for LLG Faults in Case of Hybrid

In this chapter, here the effect of location of hybrid system (PV and TYPE-3 WTG) on short circuit level of IEEE-37 distribution system by using Etap software is examined. The amount of fault contributed by different type of DG is depends on no. of factors which is explained in chapter 3. Here SCC values shown in above table 5.2 are rms values of fault current during 1.5 to 4 cycles. 2. The impact of different types of fault on the short circuit level in Hybrid system for all scenarios applied follows the same sequence as in case of WTG or PV but the change in the SCL is significant (around 0.5-6 %) for scenarios 2 to 6 in comparison with scenario 1 as shown in Figure 5.2-5.5 above.

5.4 CONCLUSIONS

In this chapter the impact of Hybrid DG penetration on the SCL of IEEE 37-bus distribution system by comparing different scenarios for all four types of fault is analysed. The impact of different types of fault on the SCL in Hybrid system shows the same behaviour as in case of Type-3 wind turbine or PV explained in chapters 3 and 4. But the contribution of Hybrid renewable energy system to SCL was moderate i.e between Type-3 wind turbine and PV.

CONCLUSION

This thesis examined the effect of DG allocation and penetration on the fault current of IEEE 37-bus system. Comparing the impact of different types of DG used, it is observed that the Type-3 wind turbine generator has the most significant impact, followed by the Hybrid (PV and WTG Type-3) case and PV has the least significant impact on SCL. From this we can conclude that the impact of PV on SCL is negligible compared to the two other scenario of the DG connection. And out of four different types of fault 3-ph fault has most significant effect and LG fault has least effect. SCL is highest for a fault near the grid and least at the farther bus location from grid for all the six scenarios. It is also observed that the DG penetration level is directly dependent on fault current contributed by the DG at the selected bus.

APPENDIX-A

CALCULATION OF SCC OF WIND TURBINES

Determination of fault current contributed by different wind turbine is explained here, as calculation SCC for variable-speed WTG with PEC between stator and grid is relatively easy, which is determined by converter and generally it will not exceed the (nominal) current rating of converter. Wind turbines like constant-speed and a variable-speed turbine with DFIG, both have grid connected induction machine. The SCC behaviour of induction machines is depends on characteristics of machine[23]. A DFIG is directly grid coupled and it also have PEC between rotor and grid . To determine the maximum short-circuit current some good approximate equations have been derived [38]. Here a worst case is considered in which a short circuit occurs at the terminals of the induction machine.

Induction Machine Response to Fault

Here we determines the response of machine to 3-ph fault at its stator terminals which is based on [38]. Equations which explains an induction machine in a synchronously rotating reference frame are [38]

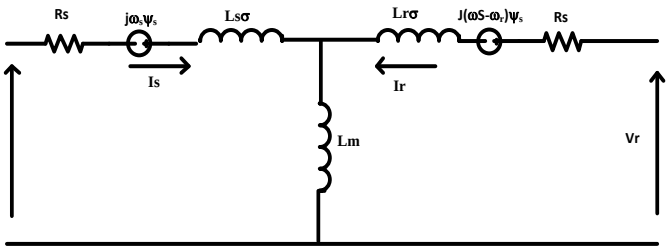

Figure 1. Equivalent circuit of IM

$$v_s = R_s i_s + \frac{d\psi_s}{dt} + j\omega_s \psi_s \ldots\ldots\ldots\ldots\ldots\ldots\ldots\ldots(1)$$

$$v_r = R_r i_r + \frac{d\psi_r}{dt} + j(\omega_s - \omega_r)\psi_r \ldots\ldots\ldots\ldots\ldots(2)$$

$$\psi_s = L_s i_s + L_m i_r \ldots\ldots\ldots\ldots\ldots\ldots\ldots\ldots\ldots\ldots\ldots(3)$$

$$\psi_r = L_m i_s + L_r i_r \text{.....(4)}$$

Where symbols represents - f –Freq. [Hz] , i -Current [A], I -phase current [A], k- Coupling factor , L- Inductance [H],R- Resistance [Ω], t- Time [s], T- Time constant [s], v- Voltage [V], V- Effective phase voltage [V], X- Reactance [Ω], Z- Impedance [Ω], α- Angle [rad], σ- Leakage factor, ω- Angular velocity [rad/s], ψ- Flux [T] and Subscripts a- Phase a, cb- Crowbar, m- Mutual, max- Maximum, r- Rotor, s- Stator and σ- Leakage.

In above equations, parameters are expressed to the stator side. On the basis of equations, the equivalent circuit of IM is shown above in Figure , which may be used for transient analysis of IM. From (3) and (4), the currents can be expressed as

$$i_s = \frac{1}{L_s - \frac{L_m^2}{L_r}} \psi_s - \frac{L_m}{L_r} \frac{1}{L_s - \frac{L_m^2}{L_r}} \psi_r \text{.....(5)}$$

$$i_r = -\frac{L_m}{L_s} \frac{1}{L_r - \frac{L_m^2}{L_s}} \psi_s + \frac{1}{L_r - \frac{L_m^2}{L_s}} \psi_r \text{.....(6)}$$

Term $L_s - \left(\frac{L_m^2}{L_s}\right)$ represents transient inductance which is denoted as L'_s. As $L_s = L_{s\sigma} + L_m$ and $L_r = L_{r\sigma} + L_m$, so transient stator inductance may be expressed as

$$L'_S = L_{S\sigma} + \frac{L_{r\sigma} L_m}{L_{r\sigma} + L_m} \text{.....(7)}$$

In the same way, the transient rotor inductance expressed as

$$L'_r = L_{r\sigma} + \frac{L_{S\sigma} L_m}{L_{S\sigma} + L_m} \text{.....(8)}$$

Introducing coupling factor of stator and rotor equations can be simplified as

$$k_s = \frac{L_m}{L_s} \text{.....(9)}$$

$$k_r = \frac{L_m}{L_r} \text{.....(10)}$$

and the leakage factor as

$$\sigma = 1 - \frac{L_m^2}{L_s L_r} \ldots\ldots\ldots\ldots\ldots\ldots\ldots\ldots\ldots\ldots\ldots\ldots\ldots\ldots(11)$$

With the inductances and factors, (5) and (6) become

$$i_s = \frac{\Psi_s}{L_s'} - k_r \frac{\Psi_r}{L_s'} \ldots\ldots\ldots\ldots\ldots\ldots\ldots\ldots\ldots\ldots\ldots\ldots(12)$$

$$i_r = -k_s \frac{\Psi_s}{L_r'} + \frac{\Psi_r}{L_r'} \ldots\ldots\ldots\ldots\ldots\ldots\ldots\ldots\ldots\ldots\ldots(13)$$

Amount of current supplied by an IM will be approximated using above equations. The voltage equations of an induction machine are given by (1) and (2). Solving differential equations 1 and 2 give the current in a steady-state situation.

During the occurrence of a short circuit, currents are present in the induction machine are Stationary current having frequency of f_s (stator) and $f_r = sf_s$ (rotor), Stator dc current:as the rotor rotates with $\omega_m = (1-s)\omega_s$ (one pole pair) w.r.t this fixed space vector, the rotor adds an alternating current with $f = (1-s)\omega_s$ to this dc current and Rotor dc current which rotates with rotor and creates the a.c in stator.

Actually there is no real dc currents in dc components. The space vector slowly rotates and damped exponentially. The time constant for stator and rotor is [38]

$$T_S' = \frac{L_S'}{R_S} \ldots\ldots\ldots\ldots\ldots\ldots\ldots\ldots\ldots\ldots\ldots\ldots(14)$$

$$T_r' = \frac{L_r'}{R_r} \ldots\ldots\ldots\ldots\ldots\ldots\ldots\ldots\ldots\ldots\ldots\ldots(15)$$

SCC of an idle machine is determined (neglecting mechanical losses, rotational speed ω_s.).For steady state stator resistance can be neglected. Before short circuit, the rotor current is zero $I_r = 0$. The stator current is

$$I_s e^{j\omega_s t} = \frac{V_s e^{j\omega_s t}}{jX_s} = \frac{V_s e^{j\omega_s t}}{j\omega_s L_s} \ldots\ldots\ldots\ldots\ldots\ldots\ldots\ldots(16)$$

The stator flux is

$$\psi_s e^{j\omega_s t} = I_s e^{j\omega_s t} L_s = \frac{V_s e^{j\omega_s t}}{j\omega_s} \ldots\ldots\ldots\ldots\ldots\ldots\ldots\ldots(17)$$

The rotor flux is

$$\psi_r e^{j\omega_s t} = I_s e^{j\omega_s t} L_m = \frac{L_m}{L_s} \frac{V_s e^{j\omega_s t}}{j\omega_s} = k_s \frac{V_s e^{j\omega_s t}}{j\omega_s} \ldots\ldots(18)$$

Three-phase short circuit is assumed to occur at t=0 at stator. So rotor and stator are short circuited, which implies that there is no change in flux. The stator flux is given by

$$\Psi_s = \Psi_{s,0} = \frac{\sqrt{2}V_s}{j\omega_s} \ldots\ldots\ldots\ldots\ldots\ldots\ldots\ldots\ldots\ldots\ldots(19)$$

See figure -2 ,the rotor flux is thus given by

$$\psi_r = \psi_{r,0} = k_s \frac{\sqrt{2}V_s}{j\omega_s} e^{j\omega_s t} \ldots\ldots\ldots\ldots\ldots\ldots\ldots\ldots\ldots\ldots(20)$$

During short circuit, rotor and stator flux ψ_r and ψ_s have same angle and amplitude. The stator flux is fixed, but rotor flux will change with rotor and after half time, become 180° out of phase.

Stator SCC is obtained by putting (19) and (20) in (12) as

$$i_s = \frac{\psi_s}{L_s'} - k_r \frac{\psi_r}{L_s'} = \frac{\psi_s - k_r\psi_r}{L_s'} = \frac{\sqrt{2}V_s}{j\omega_s L_s'}\left[1 - k_r k_s e^{j\omega_s t}\right] \ldots\ldots\ldots\ldots(21)$$

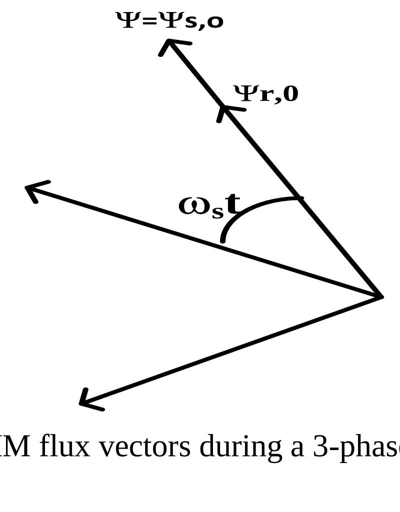

Figure -2. IM flux vectors during a 3-phase short circuit.

Writing $k_r k_s$ as $1-\sigma$ [see (9)–(11)], the equation becomes

$$i_s = \frac{\sqrt{2}V_s}{j\omega_s L_s'}\left[1 - (1-\sigma)e^{j\omega_s t}\right] \ldots\ldots\ldots\ldots\ldots\ldots\ldots\ldots\ldots\ldots(22)$$

Above equation is obtained (stator and rotor resistance neglected), implying that the current is un-damped but in reality it will decline. Here first term represents dc

component in stator current which damped with time constant T_s'. The second term represents ac component in stator current and damped with time constant T_r'. So equation (22) becomes [38].

$$i_s = \frac{\sqrt{2}V_s}{jX_s'}\left[e^{-\frac{t}{T_s'}} - (1-\sigma)e^{j\omega_s t}e^{-\frac{t}{T_r'}}\right]\ldots\ldots\ldots\ldots\ldots\ldots\ldots\ldots\ldots\ldots(23)$$

When the voltage v_s has angle $\alpha + (\pi/2)$ with respect to stator phase a at the moment of short circuit, then $v_s = \sqrt{2}V_s e^{ja}$. The SCC is then projection of the vector on the a-phase, i.e., its real part

$$i_{sa} = \frac{\sqrt{2}V_s}{X_s'}\left[e^{-\frac{t}{T_s'}}\cos\alpha - (1-\sigma)e^{j\omega_s t}e^{-\frac{t}{T_r'}}\cos(\omega_s t + \alpha)\right]\ldots\ldots\ldots(24)$$

The current after half a period $t = T/2$ gives appox. of the maximum current [38]. The maximum current is therefore

$$i_{s\,max} = \frac{\sqrt{2}V_s}{X_s'}\left[e^{-\frac{T}{2T_s'}} + (1-\sigma)e^{-\frac{T}{2T_r'}}\right]\ldots\ldots\ldots\ldots\ldots\ldots\ldots\ldots\ldots\ldots\ldots\ldots(25)$$

Calculate the maximum SCC of DFIG by putting the values of T_r' from table -1 as observed from figure-5 by using above equation (25). In the same way SCC values for other type of WTG can also be calculated using table-1.

Equivalent circuit of various WTG for short circuit analysis

Equivalent circuit diagram of various type of wind turbine like type-1, type-2, type-3 are shown respectively in figure 3, 4 and 5 for short circuit analysis of turbines under fault condition [37].

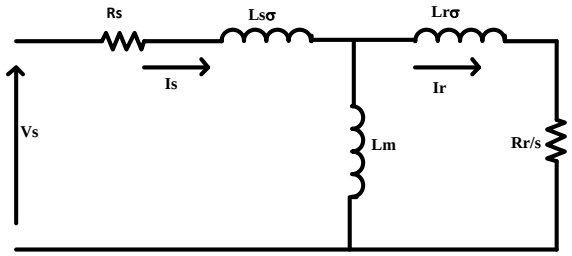

Figure -3 Equivalent circuit diagram of a Type 1wind turbine

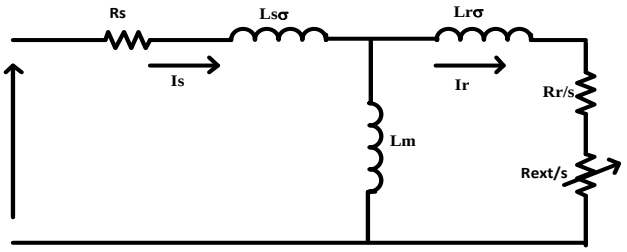

Figure -4 Equivalent circuit diagram of a Type 2 wind turbine

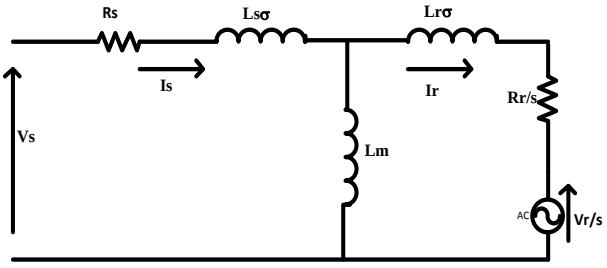

Figure-5 Equivalent circuit diagram of a DFIG

TABLE-1 TIME CONSTANT AND IMPEDANCE VALUES FOR DIFFERENT TYPES OF WTGS

WTG	**TYPE-1**	**TYPE-2**	**TYPE-3**
Z'_S	$X'_S = \omega L'_S$	$\sqrt{X'^2_S + R^2_{ext}}$	$\sqrt{X'^2_S + R^2_{CB}}$
T'_r	$\frac{L'_r}{R_r}$	$\frac{L'_r}{R_r + R_{ext}}$	$\frac{L'_r}{R_r + R_{CB}}$

TABLE-2 MAXIMUM AND MINIMUM POSSIBLE VALUE OF THE SCC

WTG	**TYPE-1**	**TYPE-2**	**TYPE-3**	**TYPE-4**
MAX I_{SC} PEAK	$2\frac{\sqrt{2}V_S}{X'_S}$	$2\frac{\sqrt{2}V_S}{X'_S}$	$2\frac{\sqrt{2}V_S}{X'_S}$	1.1 I_{RATED}
MIN I_{SC} PEAK	$\frac{\sqrt{2}V_S}{X'_S}$	$\frac{\sqrt{2}V_S}{\sqrt{X'^2_S + (9R'_r)^2}}$	1.1 I_{RATED}	0

Table I shows the parameters that are used to put in above equations for calculation of SCC for various types of WTGs. In Table II [37] the max. and min. values of peak of SCC is shown. As observed from above that the Type 1 may produce the largest SCC. Its max. value depends AC peak and the highest DC component value, and the min. value is depends on AC peak only. It is also observed from table 1 and 2 the SCC contribution for type-4 WTG is limited to its rated current as it is designed with an overload capability of 10% [26],[37].

APPENDIX-B

SHORT CIRCUIT ANALYSIS OF PV

The PV represents fastest growing source of energy(renewable) worldwide. By 'Photovoltaic effect' we can directly convert sunlight into energy (electrical) which occur by photovoltaic cell. By grouping PV cells module is formed. And therefore number of modules are connected in a series-parallel configuration to produce the required amount of power. Output power of array is affected by conditions such as location, irradiance, and temperature as explained in chapter 1. Figure 4.2 shows a basic PV system .The PV modules interconnected via inverters, to convert the DC into AC power.

Grid connected PV operates in parallel and interconnected to grid. Figure 4.2 shows a fundamental PV power system. So to analyse the impact of grid connected PV on electrical power system we model the PV system as shown in figure -1, where ac voltage input represents the output of inverter , elements L & C represents the LC filter of inverter and R is the load resistance. In parallel to load resistance breaker is connected to analyse the impact of short circuit.

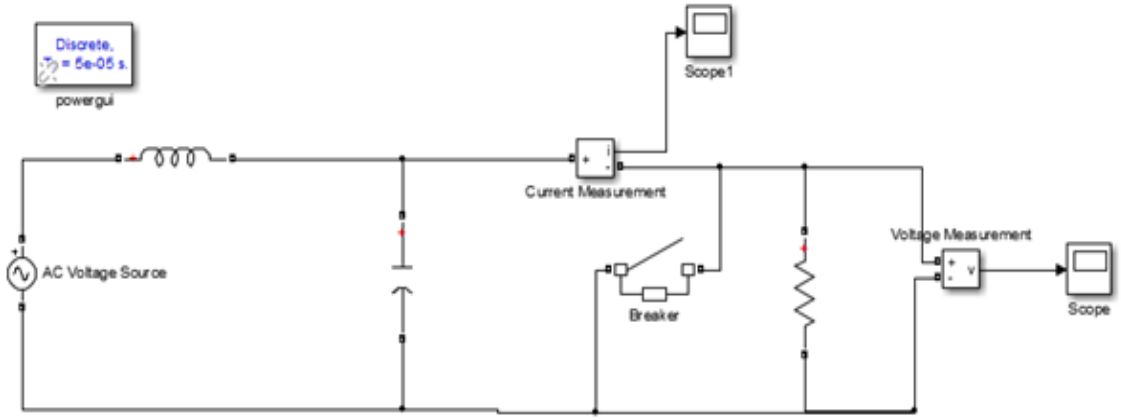

Figure-1 Equivalent circuit diagram of pv inverter

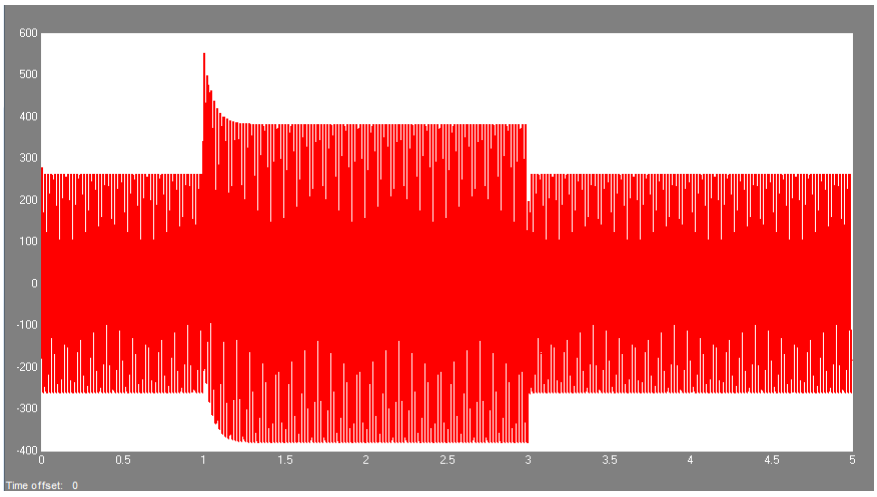

Figure -2 represents the fault current value for t =1to t = 3 sec

While experiment, inverters are shown to contribute a small short current transient during faults. Transient is less than 250% of peak rated inverter current and exists for few cycles only as observed in figure-2 when short circuit is observed for 2 second. So it validates that the fault contributed by inverter-based system contain a “a rule of thumb” of one to two times an inverter’s full load current for few cycles [1].

REFERENCES

[01] J. Keller, B. Kroposki "Understanding fault characteristics of Inverter-Based distributed energy resources" technical report NREL/TP -550-46698, 2010.

[02] J. Moren and S.W.H. de Haan, "Short-circuit current of wind turbines with doubly fed induction generator," IEEE Trans. Energy Convers., vol. 22 Mar. 2007.

[03] Short, T.A. Electrical Power Distribution Handbook, 2004.

[04] IEEE. IEEE Std. 399-1997 Brown Book – Power System Analysis.

[05] Dugan, R., Zavadil, R.,Van Holde, D. Interconnection Guidelines for Distributed Generation. E-Source, 2002.

[06] S.N. Afifi; H. Wang; G.A. Taylor; M.R. Irving, "Impact of DFIG wind turbines on short circuit levels in distribution networks using ETAP," 48th International Universities' Power Engineering Conference, Dublin, Sep. 2-5, 2013, pp. 1-4.

[07] Begovic, M.Pregelj, A. Rohatgi, A.Novosel, D. "Impact of Renewable Distributed Generation on Power Systems." Presented at the 34th Annual Hawaii International Conference on System Sciences. (HICSS-34) Volume 2, 2001.

[08] IEEE. IEEE Std. 551-2006 Violet Book – Recommended Practice for Calculating Short-Circuit Currents in Industrial and Commercial Power Systems

[09] IEEE. Static Power Converters of 500 kW or Less Serving as the Relay Interface Package for Non- Conventional Generators, IEEE Transaction on Power Delivery, 1994

[10] Kroposki, B.Pink, C. DeBlasio, R.Thomas, H.Simoes, M.; Sen, P.K. "Benefits of Power Electronics Interfaces for Distributed Energy Systems." IEEE Power engg. Society, 2006.

[11] Kroposki, B., Optimization of Distributed and Renewable Energy Penetration in Electric Power Distribution Systems, Submitted Thesis to CSM for partial degree of Doctor of Philosophy (Engineering Systems), Golden, Colorado 2008.

[12] Kersting, W.H. and Dugan, R.C. “Recommended Practices for Distributed System Analysis.” IEEE Transaction, 2006.

[13] Boljevic, S.; Conlon, M.F., "The contribution to distribution network short-circuit current level from the connection of distributed generation," 43rd International Universities Power Engineering Conference, Padova, Sep. 1-4, 2008, pp. 1-6.

[14] E. Gursoy and R. A. Walling, “Representation of variable speed wind turbine generators for short circuit analysis,” Electrical Power and Energy Conference, Winnipeg, MP, Oct. 3-5, 2011.

[15] B. Wu, Y. Lang, N. Zargari and S. Kouro, Power Conversion and Control of Wind Energy Systems. Wiley-IEEE Press, 2011.

[16] S.N. Afifi, M.K. Darwish, G.A. Taylor, "Impact of photovoltaic penetration on short circuit levels in distribution networks," International Conference on Renewable Energy and Power Quality Conference, 2014.

[17] F. M. Hughes, O. Anaya Lara, N. Jenkins, and G. Strbac, “Control of DFIG-based wind generation for power network support,” IEEE Trans. Power Syst., vol. 20, no. 4, pp. 1958–1966, Nov. 2005.

[18] R. Zavadil, N.Miller, A.Ellis, and E.Muljadi, “Making connections [wind generation facilities],” IEEE Power Energy Mag., vol. 3, no. 6, pp. 26–37. 2005.

[19] J. Morren, J. T. G. Pierik, S. W. H. de Haan, and J. Bozelie, “Grid interaction of offshore wind farms. Part 1. Models for dynamic simulation,” Wind Energy, vol. 8, no. 3, pp. 265–278, 2005.

[20] “Grid interaction of offshore wind farms. Part 2. Case study simulations,” Wind Energy, vol. 8, no. 3, pp. 279–293, 2005.

[21] K. Maki, S. Repo, and P. Jarventausta, “Effect of wind power based distributed generation on protection of distribution network,” in Proc. 8th Inst. Elect. Eng. Int. Conf.Dev. Power Syst. Protection, vol. 1, 2004.

[22] G. C. Paap, F. Jansen, and F. K. A. M. Wiercx, “The influence of voltage sags on the stability of 10 kV distribution networks with large-scale dispersed co-generation and wind generators,” in Proc. 16th Int. Conf. Exhib. Elect. Distrib., vol. 4, 2001.

[23] J. Morren, J. T.G.Pierik, and S.W. H. de Haan, “Voltage dip ride-through of direct-drive wind turbines,” presented at the 39th Int. Univ. Power Eng. Conf., Bristol, U.K, 2004.

[24] T. N. Boutsika and S. A. Papathanassiou, "Short-circuit calculations in networks with distributed generation," Electric Power Systems Research, Vol. 78, No. 7.

[25] Barghi, Siamak; Golkar, Masoud Aliakbar; Hajizadeh, A., "Impacts of distribution network characteristics on penetration level of wind distributed generation and voltage stability," 10th International Conference on Environment and Electrical Engineering.

[26] Eduard Muljadi, Jun Li, “Short circuit current contribution for different wind turbine generator type,” IEEE Power and Energy Society, Minneapolis, MN, 2010.

[27] Baghaee, H. R.; Mirsalim, M.; Sanjari, M. J.; Gharehpetian, G.B., "Effect of type and interconnection of DG units in the fault current level of distribution networks," 13th Power Electronics and Motion Control Conference, Poznan, Sep.1-3, 2008, pp. 313-319

[28] M.Ntshangase, S.K.Kariuki, S.Chodhury “ voltage stability analysis of electricity network with DFIG –based wind power plants”10th International Conference on Environment and Electrical Engineering 2012.

[29] “Radial distribution test feeders”IEEE transactions on power system , vol.6.no.3 august 1991.

[30] Yun Tiam Tan; Kirschen, D.S., “Impact on the Power System of a Large Penetration of Photovoltaic Generation,” Power Engineering Society General Meeting, Tampa, FL, June 24-28, 2007, pp. 1-8. STATCOM,” Vehicle Power and Propulsion Conference, Seoul, Korea, October 9-12, 2012, pp. 9-12.

[31] M.Gheydi, Farshid Adbolahejad Baroogh “ comparative assessment of DFIG and Full converter generator wind turbines on short circuits in distribution systems” International Conference on Renewable Energy and Power Quality Conference,2015.

[32] https://en.wikipedia.org/wiki/Solar_power_in_India.

[33] https://en.wikipedia.org/wiki/Wind_power_in_India.

[34] “Characteristics of Wind Turbine Generators for Wind Power Plants” by IEEE PES wind plant collector system design working group.

[35] Gao Jingde, Wang Xiangheng, Li Fahai, “Analysis of AC Machine System” (second edition). Beijing: Tsinghua University Press, 2005.

[36] Li Jing, Wang Weisheng, Song Jiahua, “Modeling and Dynamic Simulation of Variable Speed Wind Turbine,” Power System Technology. vol. 27 (9),pp14-17, 2003

[37] Eduard Muljadi, Jun Li, “Short circuit modeling of wind power plant,” IEEE Power and Energy Society, Minneapolis, MN, 2010.

[38] K. P. Kov´acs and I. R´acz, Transiente Vorg¨ange in Wechselstrommaschinen–Band II. Budapest: Verlag der Ungarischen Akademie derWissenschaften, 1959, (in German).

[39] J. Niiranen, “Voltage dip ride through of doubly-fed generator equipped with active crowbar,” presented at the NordicWind Power Conf., Gothenburg, Sweden, Mar. 1–2, 2004.

[40] A. Perdana, O. Carlson, and J. Persson, “Dynamic response of grid connected wind turbine with doubly fed induction generator during disturbances,” presented at the Nordic Workshop Power Ind. Electron. (NORPIE 2004), Trondheim, Norway, 2004.